

RESEARCH

Open Access



The transcription factor PITX1 cooperates with super-enhancers to regulate the expression of DUSP4 and inhibit pyroptosis in pulmonary artery smooth muscle cells

Jingya Zhang^{1†}, Yuyu Song^{1†}, Xinru Wang¹, Xu Wang¹, Songyue Li¹, Xinyue Song², Chong Zhao³, Jing Qi¹, Yunyun Tian⁴, Baoshan Zhao⁵, Xiaodong Zheng^{6*}  and Yan Xing^{1*}

Abstract

Background Pulmonary hypertension (PH) is a highly fatal pathophysiological syndrome. The group 1 pulmonary arterial hypertension (PAH) is characterized by acute pulmonary vasoconstriction and chronic vascular remodeling caused by hyperplasia and hypertrophy of pulmonary artery smooth muscle cells (PASMCs) and chronic inflammation. Pyroptosis is an inflammatory mode of cell death that is regulated by super-enhancers (SEs) and occurs in the setting of tumors and cardiovascular diseases. However, whether SEs are involved in the pathological process of pyroptosis in PAH and the specific mechanism involved remain unclear.

Methods Here, we identified the SE target gene *DUSP4* via ChIP-seq with an anti-H3K27ac antibody, and bioinformatics predictions revealed that the transcription factor PITX1 can bind to the promoter and SE sequences of *DUSP4*. The AAV5 vector was used to deliver shRNAs targeting PITX1 and *DUSP4* to PASMCs.

Results PITX1 overexpression reversed the increase in right ventricular systolic pressure and pulmonary vascular remodeling, restored the PAAT/PAVT1 ratio in hypoxic pulmonary hypertension (HPH, Group 3 PH) and SuHx PAH (Group 1 PAH) mice, and suppressed pyroptosis in pulmonary vascular cells. However, knockdown of *DUSP4* counteracted the effects of PITX1 overexpression. Similar results were obtained in cultured PASMCs. In addition, treatment with the SE inhibitors JQ1 and iBET decreased the transcription of *DUSP4* and increased the expression of hypoxia-induced pyroptosis proteins in PASMCs.

Conclusion We confirmed that PITX1 can promote *DUSP4* expression by binding to the *DUSP4* promoter and SE to reduce pyroptosis in hypoxic PASMCs, providing new insights into the role of SEs and pyroptosis in pulmonary vascular remodeling and a theoretical basis for the treatment of PAH and related diseases.

Keywords Super-enhancer, PITX1, Pyroptosis, Pulmonary arterial hypertension

[†]Jingya Zhang and Yuyu Song have contributed equally to this work.

*Correspondence:

Xiaodong Zheng
zhengxiaodong@hmdq.edu.cn

Yan Xing
xingyan@hmdq.edu.cn

Full list of author information is available at the end of the article



Introduction

Pulmonary arterial hypertension (PAH) comprises of diverse diseases that result in similar pathological changes including continuous pulmonary vasoconstriction and pulmonary vascular remodeling in pulmonary vasculature [1], which result in an abnormally elevated pulmonary artery pressure [2]. In general, the structural remodeling of pulmonary arteries may be explained primarily by the phenotypic alteration of pulmonary artery smooth muscle cells (PASMCs) [3, 4]. Studies have reported that PASMCs pyroptosis promotes pulmonary vascular fibrosis and accelerates the development of PAH [5].

Super-enhancers (SEs) are composed of large clusters of highly active enhancers that drive intracellular expression of key genes [6]. SEs can be identified by analyzing H3K27ac enrichment via Rank Ordering of SEs (ROSE) software [7]. SEs, compared with typical enhancers (8–20 kb vs. a median of 0.8 kb). SEs display higher levels of, are characterized by more significant H3K27ac and H3K4me1 modifications and greater occupancy of the mediator (MED) complex. MED and bromodomain-containing protein 4 (BRD4) bind to and are enriched on high-density transcription factors, which have a strong regulatory effect on gene expression [8, 9]. Meanwhile, as evidenced previously, SEs have been reported to activate gasdermin D (GSDMD)-mediated pyroptosis by attenuating the expression of the histone-lysine N-methyltransferase 2D (KMT2D). Furthermore, the SE-associated circLrch3 was found to have a role in the formation of an R loop with its host gene Lrch3, which would further modulate the expression of pyroptosis-related proteins and interfere with the cellular pyroptosis process, ultimately facilitating the progression of PAH [10, 11].

As a transcription factor belonging to the pitx family, Paired-like Homeodomain 1 (PITX1) has proven to participate in various biological processes embryonic development, cell differentiation and tissue regeneration [12, 13]. PITX1 regulates the expression of target genes by recognizing a specific DNA sequence (TTAATCCC) [14]. In terms of its role as a tumor suppressor, PITX1 was reported to be highly expressed in breast cancer tissues, which could bind to the promoter of *TP53*, a tumor suppressor gene as well, to induce p53 expression and cell apoptosis [15]. Moreover, PITX1 has been identified as a transcription factor for sex-determining region Y box protein 9 (SOX9) in melanoma and shown to play an inhibitory role in cell proliferation [16]. It has been suggested that PITX1 is involved in regulating cell phenotype changes by binding to specific DNA sequences [17]. In addition, PITX1 can mediate HIF-1 α expression under hypoxic conditions [18]. PASMCs have been tested

with upregulated expression of HIF-1 α , a well-known key factor in pulmonary vascular remodeling [19]. Whether PITX1 affects PASMCs pyroptosis by binding to the SEs of key PAH genes remains unclear so far, which may be a topic of interest and deserve further investigation.

DUSP4 is a crucial protein phosphatase that dephosphorylates crucial signaling molecules and mediates the inactivation of MAPKs by dephosphorylating threonine or tyrosine residues in their activation loops [20]. MAPKs are involved in the proliferation, migration, apoptosis, and pyroptosis of pulmonary vascular cells [21, 22]. Concerning the documented roles of DUSP4 in affecting cell phenotype changes to mediate disease development. For example, decreased expression of DUSP4 promotes the proliferation, migration, and invasion of tumor cells in melanoma [23], lung cancer [24], and endometrial cancer [25]. It is also detected with downregulated expression in myocardial ischemia–reperfusion [26] and acute lung injury [27]. On the contrary, DUSP4 was highly expressed to stimulate cell proliferation and invasion in esophageal squamous cell carcinoma [28], colorectal cancer [29] and clear cell renal cell carcinoma [30]. Collectively, DUSP4 may exhibit varied expressions under the impact of different pathological factors, resulting in different downstream effects. In addition, studies have reported that miR-122 is upregulated in the setting of myocardial ischemia–reperfusion injury and inhibits pyroptosis in cardiomyocytes by targeting DUSP4 [31]. In view of the aforementioned interpretation, this study intended to explore whether DUSP4 was associated with pyroptosis in PASMCs during the development of PAH and to explore whether DUSP4 expression was cooperatively regulated by a SE and PITX1.

Materials and methods

Animal models

The experimental animals were C57BL mice (weighing 20–30 g) purchased from the Laboratory Animal Centre, The Second Affiliated Hospital of Harbin Medical University. Mouse model of PH in this study were established by hypoxia exposure alone (Group 3 HPH) and by hypoxia exposure combined with Sugen 5416 treatment (SuHx) (Group 1 PAH). This study constructed several groups including normoxic group, hypoxic group, Sugen group, adeno-associated virus serotype 5 (AAV5) carrying shDUSP4 hypoxic group, adeno-associated virus 5 (AAV5) carrying shDUSP4 Sugen group, AAV5 carrying PITX1 hypoxic group, AAV5 carrying PITX1 Sugen group, and combined AAV5 carrying PITX1 and AAV5 carrying shDUSP4 hypoxic group. The mice were then anesthetized with tribromoethanol and infected with AAVs via dropwise nasal instillation. In AAV5

hypoxic groups, mice were subjected to three weeks of hypoxia beginning two weeks after infection. In AAV5 Sugen groups, mice underwent hypoxia treatment for two consecutive weeks and Sugen 5416 administration concurrently, followed by two weeks of reoxygenation beginning two weeks after infection. In the normoxic group, the mice were maintained under normoxic conditions (21% O₂) for 21 days. In the hypoxic groups, the mice were maintained in a hypoxic chamber (10% O₂) for 21 days. The use and housing of the mice were approved by the Institutional Animal Care and Use Committee (IACUC).

Cell culture

Primary mouse PASCs (mPASCs) were purchased from Otwo Biotech (Shenzhen) Inc. The mPASCs were cultured in DMEM containing 10% serum, passaged or plated at 80% confluence, or transfected at 60–70% confluence. The cells were subsequently incubated in a 37 °C humidified cell incubator with 5% CO₂ or in a hypoxic incubator with 5% CO₂ and 3% O₂ for 24 h before further treatment.

RNA extraction and reverse transcription–quantitative polymerase chain reaction (RT–qPCR)

After the removal of the culture medium, the model PASCs were lysed with TRIzol (Invitrogen, USA) after washing three times with PBS. Chloroform was added, and the container was inverted, shaken vigorously, and then centrifuged. Isopropanol was added to the resulting solution, which was subsequently mixed, vortexed, and centrifuged. When the supernatant was discarded, the precipitate was collected for washing with 75% ethanol, centrifugation, and air-drying at room temperature. After the measurement of RNA concentration with a microplate reader (Shimadzu Corp., Japan), total RNA (0.5 µg) was reversely transcribed with the ReverTra Ace qPCR RT Kit (Toyobo, Osaka, Japan). Finally, the mRNA expression levels were measured by PCR with the employment of a SYBR Green Real-time PCR Master Mix Kit (Toyobo) and a LightCycler 480 system (Roche, Basel, Switzerland). Each experiment was repeated 6–8 times.

The specific sequences of the primers used were as follows:

Genes [forward (F), reverse (R)]	Sequences
DUSP4-F	ctc gcc tgg ttc ctt ctt gtt agc
DUSP4-R	agt cca tct ccc gca gtt cct c
PITX1-F	act cac ttc aca agc cag cag ttg
PITX1-R	ggt ctt gaa cca gac ccg cac tc
DUSP4-P-F	ggg cac gaa gaa cga gat taa gtc c
DUSP4-P-R	gct ccg aga aac ctg aca ctg tg
DUSP4-325-F	tct gag gtg acg ctc ttc tag gc
DUSP4-325-R	cca agg gct gct gaa ctt ctg tc
DUSP4-326-F	agc aag act ccc aag cct taa agc
DUSP4-326-R	tgc cac agt tgt act ttc tcc gtt c
DUSP4-328-F	cct ggc act tgg cta aac tgg tc
DUSP4-328-R	tat gta ggt ggc tcg ctc ctt ctc

Small interfering RNAs (siRNAs), plasmid design and transfection

Cells were cultured to a confluence of 60–70%. Specific small interfering RNAs (siRNAs) obtained from IBSBIO and Lipofectamine 2000 (Invitrogen, USA) were used for transfection. The corresponding assays were conducted 24 h after transfection. The si-*PITX1* sequence was: sense: 5'-GCCUGCGGCUCAAGUCCAAGC-3'; anti-sense: 5'-UUGGACUUGAGCCGCAGGCUG-3'; and the si-*SE-DUSP4* sequence was: sense: 5'-GCAGUUUAC UUGAAGUAUACA-3'; anti-sense: 5'-UAUACUUCA AGUAAACUGCUA-3'. The plasmid was synthesized by GENECHM according to the sequence.

Western blot (WB) analysis

Proteins from tissues or cells were extracted with radioimmunoprecipitation assay (RIPA) lysis buffer, followed by protein separation using 10–12% polyacrylamide gels. Proteins were transferred from the gels to nitrocellulose membranes, which were incubated with 10% nonfat milk for 1 h. The primary antibodies were CASP1 (BOSTER, Cat.BA2220, 1:1,000), NLRP3 (CST, Cat.15101S, USA, 1:500), ASC (CST, Cat.67824S, USA, 1:1,000), IL-1β (CST, Cat.122425S, USA, 1:500), IL-18 (CST, Cat.57058S, USA, 1:1,000), GSDMD (CST, Cat.39754S, USA, 1:500), PITX1 (NOVUS, Cat.NB7160, USA, 1:500; BOSTER, Cat.A02993, 1:1,000) and DUSP4 (Abcam, Cat.ab222487, USA, 1:1,000). The control antibody was anti-β-actin (ABclonal, Cat.AC004, 1:1,000). Immunoreactivity visualization was carried out using horseradish peroxidase-conjugated secondary antibodies and an enhanced chemiluminescence (ECL) reagent (Beyotime, China).

Immunofluorescence staining

PASMCs or tissue sections were subjected to antigen retrieval in 1× sodium citrate solution at 95 °C, and fixation with 4% paraformaldehyde at room temperature for 30 min. Following washing three times with PBS, staining was performed at 37 °C for 30 min after treatment with 0.4% Triton X-100. With blockage using goat serum blocking solution for 1 h, the next step was incubation with anti-PITX1 (1:100), anti-DUSP4 (1:100), or anti-caspase 1 (CASP1) (1:100) antibody overnight at 37 °C. The next day, after another three times of washing with PBS, the cells or tissue sections were incubated with PBS-diluted fluorescent secondary antibodies (Cat. F0103B and Cat. NL004, RD SYSTEMS, USA; Cat. 711-545-152 and 715-545-151, Jackson, USA; 1:100 dilution) in dark at 37 °C for 2 h. Finally, the cells were incubated with 4',6-diamidino-2-phenylindole (DAPI) at room temperature in dark for 15 min. Images were acquired with a live cell workstation (AF6000, Leica, Germany).

Fluorescence in situ hybridization (FISH)

After digestion with 0.25% pepsin at 37 °C for 30 min, mPASMCs and mouse lung tissues were fixed with 4% paraformaldehyde for 20 min, treated with 0.5% Triton[®] X-100 for 15 min, and then hybridized with the DUSP4 probe in hybridization solution overnight at 4 °C. Staining of the nuclei with DAPI was performed after the removal of the hybridization solution. Similarly, changes in expression were observed with a live-cell workstation. The sequence of the DUSP4 probe was as follows:

(1) 5'-GCCTG CGCTC TGGCC TCTAC TCGGC TGTCA TCGTC TACGA-3'; (2) 5'-AGGCG TTGCG CCGGA ACGCG GAGCG CACGG ACATC TGCCT-3'; and (3) 5'-AGTTC GTCTT CAGCT TCCCT GTGTC TGTGG GCGTG CACGC-3'.

YO-PRO-1 (YPI)/PI staining

mPASMCs cultured in a 24-well plate at 60%–70% were subsequently transfected with the siRNA/overexpression plasmid or subjected to hypoxia for 24 h. YPI and PI (1:1000) were added separately, and the cells were incubated at 37 °C in the dark for 20 min. Images were acquired with a live cell workstation.

Lactate dehydrogenase (LDH) assay

LDH release was assessed with an LDH cytotoxicity assay kit (C0016, Beyotime). mPASMCs were cultured in a 96-well plate at a density of 60%–70% and were then transfected with the siRNA overexpression plasmid or subjected to hypoxia for 24 h. To measure LDH release,

LDH release solution in cell culture medium (1:10) was added to a 96-well plate for 1 h of incubation and centrifugation at 400×g for 5 min. Then, 120 μl of each supernatant was added to a 96-well plate, with further addition of 60 μl of substrate solution. The plate was subsequently incubated on a shaker at room temperature in the dark for 30 min. Finally, the absorbance at 490 nm was measured with a microplate reader.

Dual-luciferase reporter assay

The DUSP4-SE fragment was inserted immediately upstream of the luciferase sequence to construct the pGL3-DUSP4-SE reporter plasmid (IBSBIO). Following the transfection of PITX1 plasmid and pGL3-DUSP4-SE into mPASMCs, a specific luciferase substrate was added to make the luciferase and substrate fluoresce. Luciferase activity was determined by measuring the fluorescence intensity with a dual-luciferase reporter assay kit (RG027, Beyotime) to assess the activity of the *DUSP4-SE* and the transcriptional activity of PITX1.

Chromatin immunoprecipitation–PCR (ChIP–PCR)

A Pierce[™] ChIP Kit (Thermo Fisher, USA) and formaldehyde were used to crosslink proteins and chromatin in PASMCs, and the crosslinking reaction was terminated with glycine. Following crosslinking, the cells were subjected to RNase digestion. Chromatin was then sonicated into fragments of 500–1,000 bp, which were immunoprecipitated with antibodies specific for PITX1, H3K27ac, and H3K4me1. Furthermore, DNA was isolated from the eluate of the immunoprecipitation reaction. Genomic DNA was separated with a DNA purification kit (Beyotime) and amplified via qPCR, with primers targeting *DUSP4-SE1*, *DUSP4-SE2*, and *DUSP4-SE3*.

Small animal ultrasound and right heart catheterization

After successful PH modeling, mice were anesthetized with tribromoethanol and depilated. To measure changes in the pulmonary artery acceleration time (PAAT) and pulmonary artery velocity time integral (PAVTI), echocardiography was performed with a Vevo2100 imaging system with a 2100 MHz probe (VisualSonics, Inc., USA). After the mice were anesthetized, their right jugular vein was exposed, and a Millar catheter (Millar Instruments, Inc., Houston, Texas) was inserted. The right ventricular systolic pressure (RVSP) was recorded with a PowerLab monitoring device (AD Instruments, Colorado Springs, Colorado), and the continuous traces were averaged. Mice were euthanized under deep anesthesia for the removal and harvesting of the lung and heart tissues. This study also measured the right ventricular hypertrophy index, also called the Fulton

index [RV/(LV+S)]. The right lungs were used for Western blot and RT-qPCR, while the left lungs were fixed with 4% paraformaldehyde for paraffin embedding.

Masson's trichrome staining

The Masson's trichrome staining kit was obtained from Solarbio. Sections subjected to deparaffinization were sequentially stained with hematoxylin, ferric chloride solution, Ponceau S (Acid Red), phosphotungstic/phosphomolybdic acid and aniline blue at room temperature. The sections were subsequently washed and dehydrated with ethanol and xylene. After dehydration, the sections were mounted with neutral gum. Afterward, the sections were observed and photographed under a Nikon Eclipse 600 microscope.

Statistical analysis

In this study, GraphPad Prism software (GraphPad Software, USA) was used for statistical analysis. The normality of the data was assessed via the Shapiro-Wilk test, and a *t* test was then used for comparisons between two groups. One-way analysis of variance (ANOVA) was used for comparisons among multiple groups to evaluate the intergroup mean differences, and the Bonferroni correction was then used to correct for multiple comparisons. The data are presented as the means \pm SEMs. Statistical significance was assumed when **p* < 0.05, ** *p* < 0.01, or *** *p* < 0.001.

Results

Upregulation of the transcription factor PITX1 in hypoxic mice and PSMCs

ChIP-seq was performed by using an anti-H3K27ac antibody to screen for increased H3K27ac signals and concurrently upregulated genes in PSMCs exposed to hypoxic conditions (3% FiO₂ for 24 h) and control conditions (21% FiO₂). Increased H3K27ac signals are recognized as critical markers of SEs. Furthermore, predictions obtained via the JASPAR database revealed that most SE sequences contained binding motifs for PITX1, which showed upregulated expression under hypoxic conditions. These results suggest that PITX1 might function through interactions with these SE sequences. Consequently, we verified the expression of PITX1 in a hypoxic PH mouse model and in cultured PSMCs. Immunofluorescence staining of lung tissues sections from mice in the hypoxic PH model revealed increased expression of PITX1 and indicated that PITX1 was localized in the smooth muscle layers of pulmonary arteries (Fig. 1A, B). Western blot and RT-qPCR analyses revealed elevated PITX1 protein and mRNA expression

in the lung tissues of mice with hypoxic PH (Fig. 1C, D). mPSMCs subjected to hypoxia for 0, 6, 12, 24, and 48 h presented increased expression of PITX1 at 12, 24, and 48 h. Considering significant increase at 24 and 48 h as well as the lack of difference between these two time points, 24 h was selected as the duration of hypoxia for subsequent experiments (Fig. 1E, F). These results confirmed the upregulation of PITX1 under hypoxic conditions.

Impact of PITX1 on pyroptosis in hypoxia-induced PSMCs

A gene set enrichment analysis (GSEA) was employed to explore the importance of the increased PITX1 expression under hypoxic conditions. The results implied the function of SE in the inflammasome signaling pathway (Fig. 2A). Based on the results of siRNA interference efficiency by Western blot, siRNA segments 2 and 3 significantly inhibited PITX1 expression, and segment 2 was used for subsequent experiments (Fig. 2B); moreover, PITX1 was successfully overexpressed via plasmid transfection (Fig. 2C). Further examination of the expression of pyroptosis-related proteins in cultured PSMCs indicated increased levels of CASP1, GSDMD-N, IL-18, and IL-1 β under hypoxia. These expressions were further boosted after the knockdown of PITX1 under hypoxic conditions, but had no such effect was observed under normoxic conditions (Fig. 2D). Consistent results were observed in the YP1/PI assay, as indicated by the number of pyroptotic cells (Fig. 2E); by DiO staining, which revealed a decrease in cellular membrane integrity (Fig. 2F); and the LDH release assay (Fig. 2G). When PITX1 was overexpressed in PSMCs via plasmid transfection, overexpression of PITX1 reduced or reversed the hypoxia-induced release of LDH (Fig. 2H); increase in the levels of CASP1, GSDMD-N, IL-1 β , and IL-18 (Fig. 2I); increase in pyroptosis, as determined by the YP1/PI assay (Fig. 2J); and decrease in cellular membrane integrity, as determined by DiO staining (Fig. 2K). In contrast, overexpression in normoxic cells did not affect these pyroptosis markers. Collectively, PITX1 knockdown might exacerbate and PITX1 overexpression prevent pyroptosis in hypoxic but not normoxic PSMCs.

Overexpression of PITX1 reversed pulmonary vascular remodeling and pyroptosis in the hypoxia and SuHx mouse models

To investigate the role of PITX1 in the development of PH, PITX1 was overexpressed using AAV5 in mice through nasal instillation, after which the mice were subjected to both SuHx PAH and hypoxic PH modeling. In the SuHx PAH mouse model with PITX1

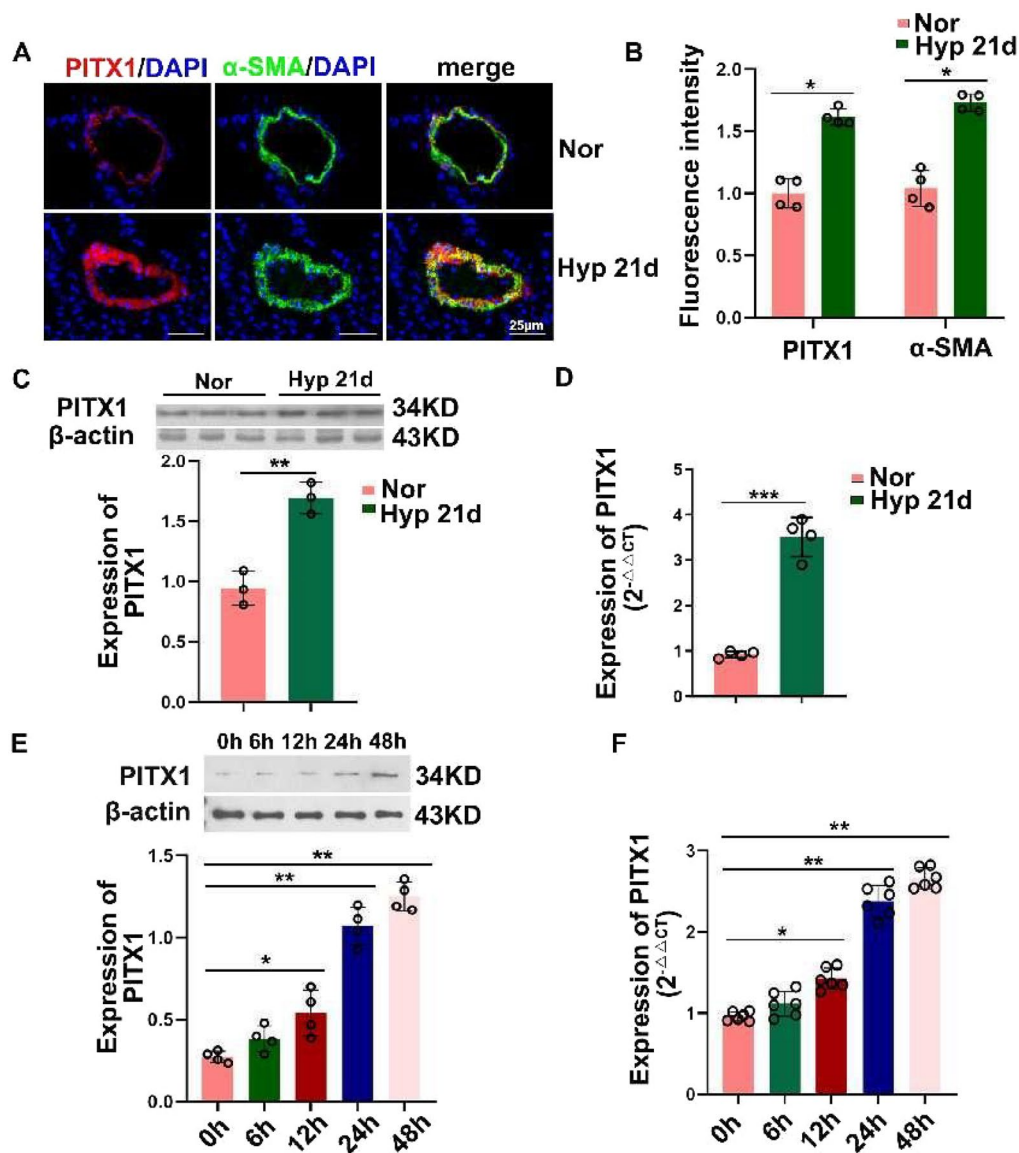


Fig. 1 Upregulation of PITX1 in hypoxic mice and PASCs. **A, B** Immunofluorescence staining: Localization and statistical data of PITX1 in tissues. Scale bar: 25 μ m. **C** Western blot: Representative image and statistical data of PITX1 expression in the lung tissues of mice. **D** RT-qPCR: Changes in the transcript level of PITX1 in the lung tissues of mice. **E** Western blot: Representative image and statistical data of PITX1 expression in the smooth muscle cells of mice. **F** RT-qPCR: Changes in the transcript level of PITX1 in the smooth muscle cells of mice. *Nor* normoxic, *Hyp* hypoxic. All values are presented as means \pm SEMs (* p < 0.05, ** p < 0.01, and *** p < 0.001; $n \geq 3$)

(See figure on next page.)

Fig. 2 Impact of PITX1 on pyroptosis in hypoxia-induced PASCs. **A** GSEA: The functions of PITX1 were enriched mainly in the inflammasome signaling pathway under hypoxic conditions. **B, C** Western blot: The interference efficiency of siPITX1 and the overexpression efficiency of the PITX1 plasmid. **D, I** Western blot: Representative images and statistical data of CASP1, GSDMD-N, IL-1 β , and IL-18 levels. **E, J** YPI/PI staining: YPI is a green fluorescent dye permeable to the membrane of apoptotic cells, and PI staining of necrotic cells with compromised membrane integrity may result in the emission of red fluorescence. Scale bar: 100 μ m. **F, K** DiO staining: Green fluorescence staining of the cell membrane; and the membranes of live cells exhibit green fluorescence. Scale bar: 50 μ m. **G, H** LDH assay: Determination of the number of dead cells by measuring the amount of LDH released from the membrane of damaged cells. *Nor* normoxic, *Hyp* hypoxic, *NC* noncoding nucleotides, *siPITX1* PITX1 siRNA, and *p-PITX1* PITX1 plasmid. All values are presented as means \pm SEMs (* p < 0.05, and ** p < 0.01; $n \geq 3$)

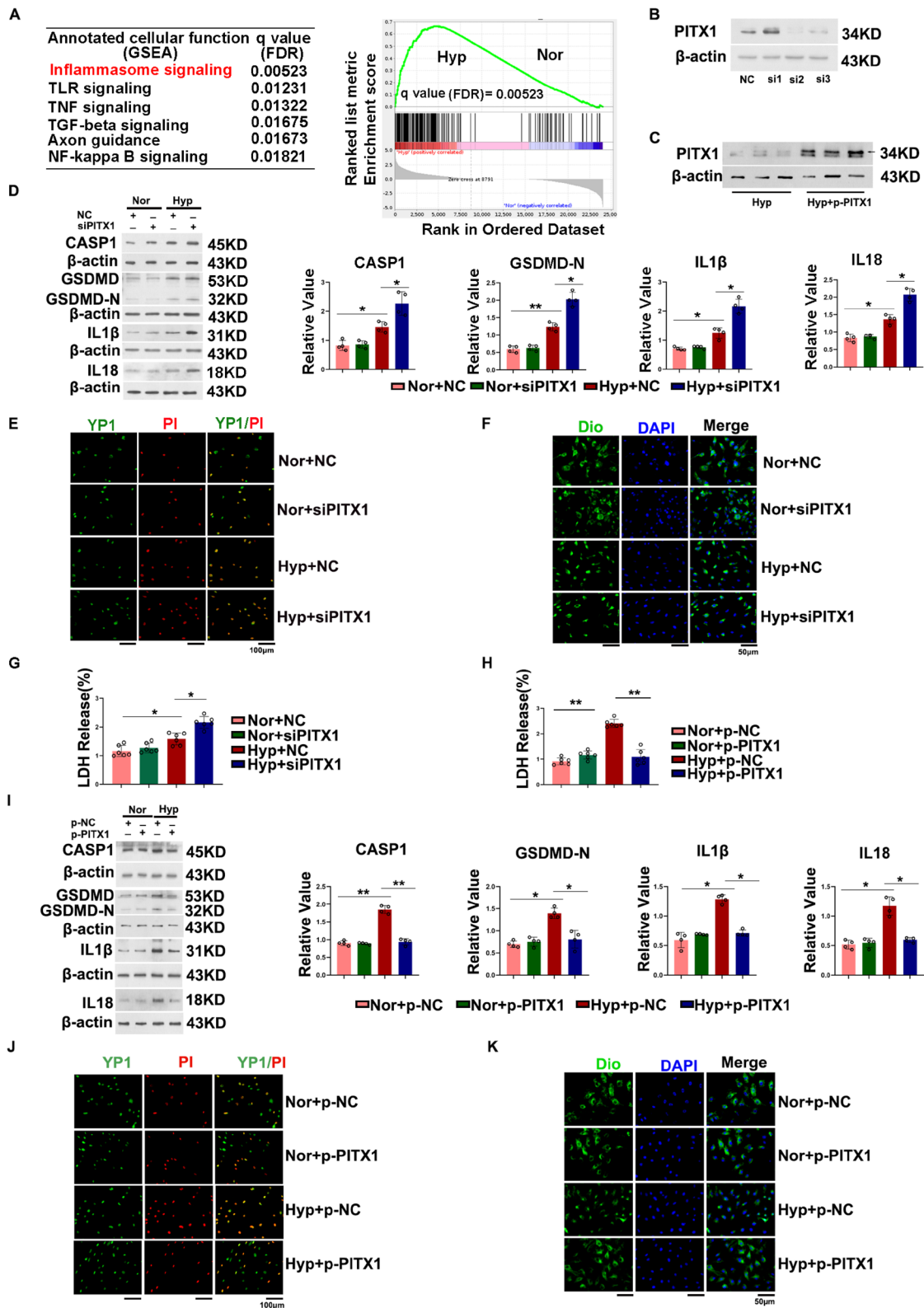


Fig. 2 (See legend on previous page.)

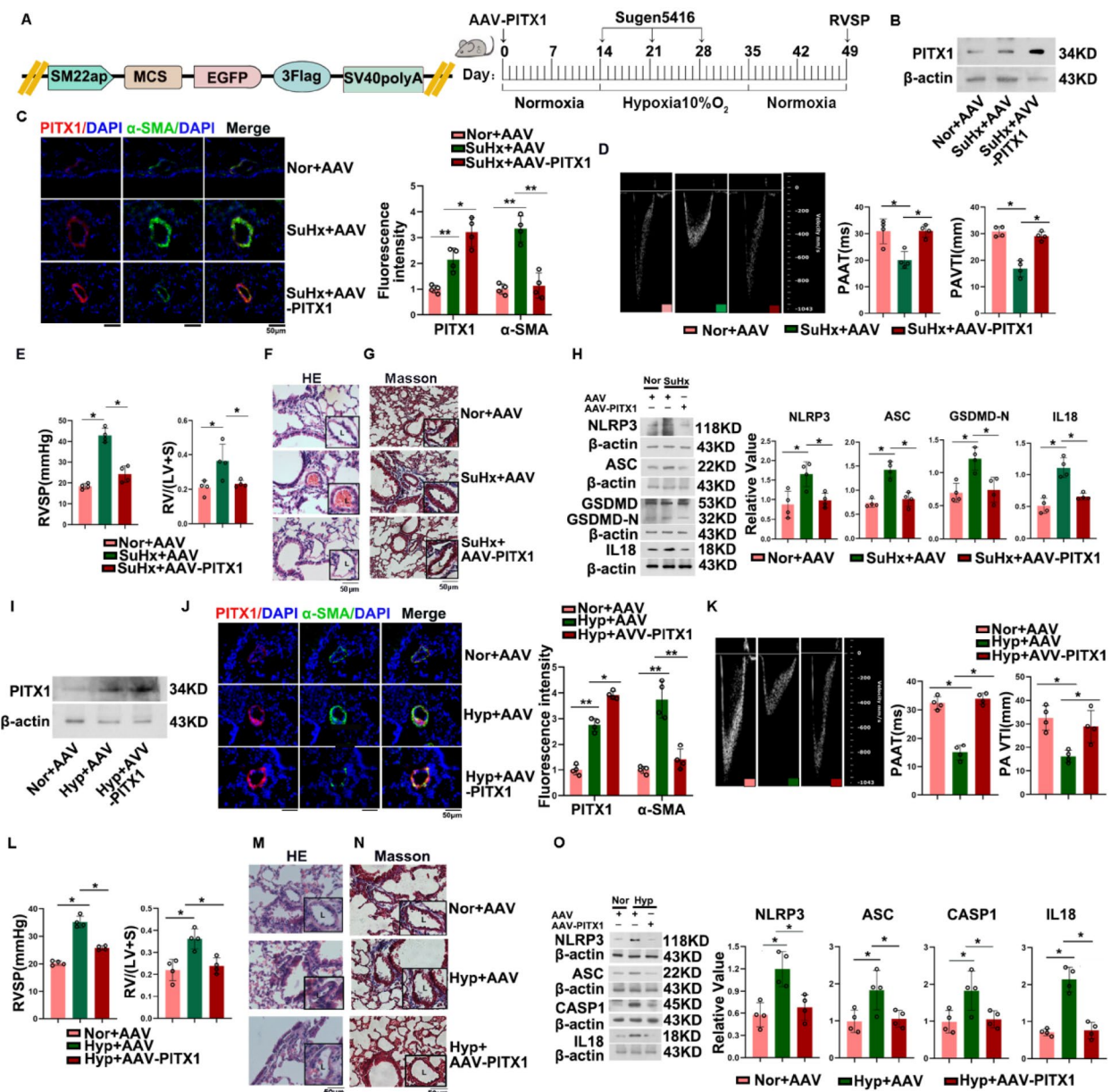


Fig. 3 Reversal of pulmonary vascular remodeling and pyroptosis in the hypoxic PH and SuHx PAH mouse models by overexpressing PITX1. **A** Construction of the PITX1 AAV5 plasmid and establishment of the SuHx PAH model under normoxic and hypoxic (10% O₂) conditions with the overexpression of PITX1 via AAV5 in mice. **B, I** Western blot: Representative images of the overexpression efficiency of PITX1 plasmid in the SuHx PAH and hypoxic groups. **C, J** Immunofluorescence staining: Overexpression of PITX1 in the SuHx PAH and hypoxic groups as well as statistical analysis. Scale bar: 50 μm. **D, K** Representative echocardiograms (left) and statistical analysis of PAAT (right 1), and PAVTI (right 2), as measured by echocardiography. **E, L** Right heart catheterization and the right ventricular hypertrophy index. **F, G, M, N** Representative images of H&E and Masson's trichrome staining in the lung tissues of the modeled mice. Scale bar: 50 μm. **H, O** Western blot: Representative images as well as statistical data of NLRP3, ASC, CASP1, GSDMD-N and IL18 levels. PAAT pulmonary artery acceleration time, PAVTI pulmonary artery velocity time integral, AAV AAV5, adeno-associated virus 5. All values are presented as means ± SEMs (*p < 0.05, and **p < 0.01; n ≥ 3)

overexpression, two weeks after intranasal instillation of AAV5, the mice received weekly injections of Sugen 5416 (for 3 weeks), followed by three weeks of hypoxia exposure and two weeks of reoxygenation (Fig. 3A). In

the hypoxic PH mouse model, beginning two weeks after intranasal administration of AAV5, the mice were housed under hypoxic conditions for three weeks. Pulmonary arteries were harvested from the modeled mice to

validate PITX1 overexpression, which were confirmed to be successful via Western blot and immunofluorescence staining (Fig. 3B, C, I, J). Echocardiography revealed significant decreases in PAAT and PAVTI in the SuHx PAH and hypoxic PH groups, and these decreases were reversed by PITX1 overexpression (Fig. 3D, K). Meanwhile, right heart catheterization demonstrated significant increase in right ventricular systolic pressure (RVSP) in the SuHx PAH and hypoxic PH groups, which were reversed by PITX1 overexpression. Similar results were observed for the right ventricular hypertrophy index ($[RV/(LV+S)]$) (Fig. 3E, L), indicating that the overexpression of PITX1 significantly ameliorated the right ventricular hypertrophy induced in the hypoxic PH and SuHx PAH mice. To assess the impact of PITX1 on pulmonary vascular remodeling, we conducted hematoxylin and eosin (H&E) and Masson's trichrome staining, which revealed that overexpression of PITX1 markedly ameliorated the vascular remodeling induced in the SuHx PAH and hypoxic PH mouse models (Fig. 3F, G, M, N). Moreover, overexpression of PITX1 inhibited the increased levels of pyroptosis-related proteins, such as NLRP3, ASC, GSDMD-N, and IL-18, in the lung tissues of SuHx PAH mice (Fig. 3H) and mice with hypoxic PH (Fig. 3O). Altogether, overexpression of PITX1 significantly inhibited vascular remodeling and pyroptosis, thereby alleviating SuHx PAH and hypoxic PH mice.

Identification of DUSP4 as a target gene regulated by SEs

A total of 1,585 genes were upregulated under hypoxic conditions, as indicated by ChIP-seq (Supplementary Fig. 1A). Among them, 50 were highly enriched with H3K27ac (Supplementary Fig. 1B). Intersection of these datasets revealed that 14 genes were both upregulated under hypoxic conditions and enriched with H3K27ac (Supplementary Fig. 1C). Subsequent analysis of these 14 genes via ROSE (Fig. 4A) and in the ChIP-seq data indicated greater H3K27ac enrichment in *DUSP4* under hypoxic conditions than under normoxic conditions. JASPAR predictions revealed that the gene sequences in H3K27ac-enriched regions, specifically *SE-DUSP4* sequences, were highly consistent with the binding motifs for PITX1 (Fig. 4B). Furthermore, dual-luciferase reporter assay revealed significantly increased luciferase activity in the presence of three segments of *SE-DUSP4* compared with that in the control group (Fig. 4C). In addition, ChIP was performed with anti-H3K27ac, anti-H3K4me1, and anti-PITX1 antibodies and qPCR was then performed with three sets of primers targeting the *DUSP4* promoter and SE regions (Fig. 4D–F). The results further confirmed that *DUSP4* expression was regulated by a SE and was dependent on PITX1.

Upregulated expression of DUSP4 inhibited vascular remodeling and pyroptosis in hypoxic and SuHx mice

To verify expression and tissue localization of *DUSP4* by immunofluorescence staining, it was found to be located primarily in the smooth muscle layer and that its expression increased under hypoxic conditions (Fig. 5A). RT-qPCR and Western blot revealed increased transcript and protein levels of *DUSP4* in the lung tissues from hypoxic mice (Fig. 5B, C). In addition, PASMCs were subjected to graded hypoxia for 0, 6, 12, 24, and 48 h, and subsequent RT-qPCR and Western blot analyses confirmed that the *DUSP4* mRNA and protein levels were increased at 12, 24, and 48 h, with the most significant increases at 24 h (Fig. 5D, E). In view of the above, *DUSP4* was knocked down in SuHx PAH and hypoxic PH mice via intranasal infection with AAV5 carrying *DUSP4* shRNA (Fig. 5F). *DUSP4* knockdown was confirmed by Western blot and immunofluorescence staining (Fig. 5G, H, N, O). Echocardiography revealed that *DUSP4* knockdown aggravated the decreases in PAAT and PAVTI in both models (Fig. 5I, P). Right heart catheterization indicated that *DUSP4* knockdown exacerbated the increase in RVSP, with similar results found for right ventricular hypertrophy index (Fig. 5J, Q). H&E and Masson's trichrome staining revealed that *DUSP4* knockdown exacerbated vascular remodeling compared to that in wild-type mice (Fig. 5K, L, R, S). Moreover, *DUSP4* knockdown significantly increased the levels of the pyroptosis proteins NLRP3, ASC, GSDMD-N, and IL-1 β in both models compared with those in the corresponding wild-type mice (Fig. 5M, T). Consequently, *DUSP4* knockdown exacerbated pulmonary vascular remodeling and tissue pyroptosis in SuHx PAH and hypoxic PH mice.

Modulating pyroptosis by influencing DUSP4 through its SE

Previous analyses, including motif analysis and ChIP-qPCR, showed that the transcription factor PITX1 could bind to the promoter and three SE sequences of *DUSP4*. Accordingly, this study further investigated the impact of SE on the expression of *DUSP4* by constructing luciferase reporter plasmids containing the three SE segments and their mutants (Fig. 6A). Dual-luciferase reporter assays revealed that cotransfection of PITX1 and the SE plasmid increased luciferase activity, whereas mutation of the SE significantly reduced luciferase activity (Fig. 6B). Cotransfection of PITX1 plasmid with the SE segments into PASMCs also revealed increased transcriptional and protein expressions of *DUSP4* (Fig. 6C, D). Therefore, PITX1 could bind to the SE sequences of *DUSP4*, thereby increasing *DUSP4* expression. To further investigate the impact of the *DUSP4* SE on pyroptosis, we treated

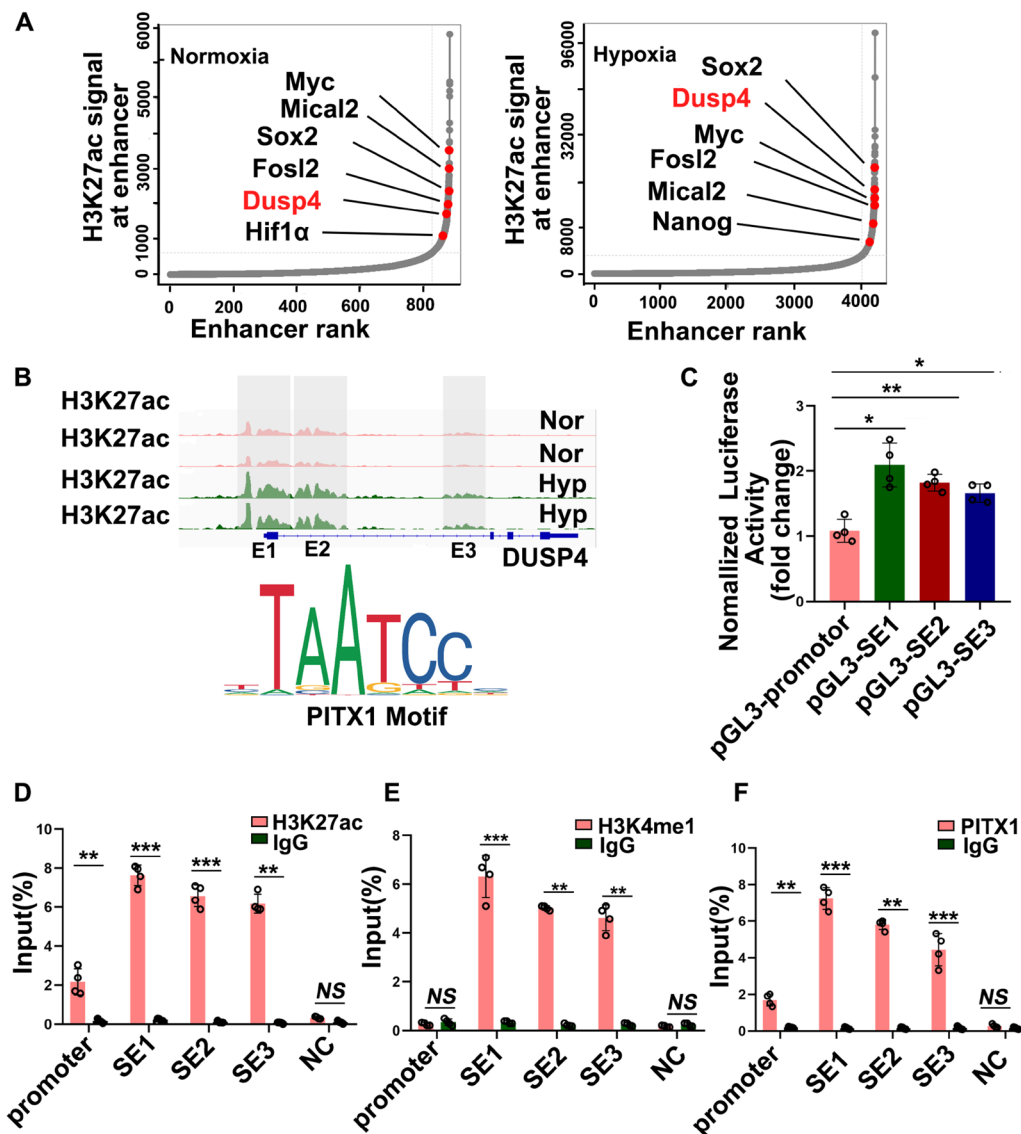


Fig. 4 Identification of DUSP4 as a target gene regulated by super-enhancers. **A** Analysis of the genes regulated by SEs under hypoxic conditions via ROSE. **B** ChIP-seq datasets to reveal increased levels of H3K27ac modification and the PITX1 binding sequence in DUSP4 under hypoxic conditions. **C** Dual-luciferase reporter assay: Luciferase activity of the DUSP4 promoter and three SE segments. **D, E, F** ChIP-qPCR analysis: Performance of ChIP with anti-H3K27ac, anti-H3K4me1, and anti-PITX1 antibodies, followed by PCR with primer sequences targeting SE. *Nor* normoxic, *Hyp* hypoxic, *NC* noncoding nucleotides. All values are presented as means \pm SEMs (* p < 0.05, ** p < 0.01, and *** p < 0.001; $n \geq 3$)

cells with the SE inhibitors JQ1 and iBET. RT-qPCR and Western blot analyses demonstrated that treatment with JQ1 and iBET led to decreases in the mRNA and protein levels of DUSP4 (Fig. 6E, F). Subsequent immunofluorescence staining for the pyroptosis marker CASP1 revealed increased percentages of CASP1-positive cells were detected in the JQ1- and iBET-treated groups compared with the hypoxia group (Fig. 6G). Additionally, increased levels of GSDMD-N, IL-18, and IL-1 β were observed in the JQ1 and iBET-treated groups

compared with the hypoxia group (Fig. 6H). Therefore, SE of DUSP4 could regulate DUSP4 expression to induce pyroptosis in PSMCs.

PITX1 modulated pulmonary vascular remodeling and pyroptosis through DUSP4

To further explore the regulatory function of the PITX1/DUSP4 axis in hypoxic PH, we coinfecting mice in the hypoxic PH model with AAV5 carrying the PITX1 overexpression plasmid and DUSP4 shRNA. An

increased trend in the PAAT/PAVTI ratio was observed after the overexpression of PITX1, which was prevented following simultaneous knockdown of DUSP4 (Fig. 7A, B). Right heart catheterization demonstrated that overexpression of PITX1 reversed the hypoxia-induced increase in RVSP, but this effect was diminished when DUSP4 was concurrently knocked down (Fig. 7C). H&E and Masson's trichrome staining indicated that overexpression of PITX1 ameliorated but simultaneous knockdown of DUSP4 exacerbated pulmonary vascular remodeling and fibrosis (Fig. 7D, E). The levels of pyroptosis-related proteins increased when DUSP4 was knocked down concurrently with PITX1 overexpression (Fig. 7F). Additionally, immunofluorescence staining with an anti-PITX1 antibody and FISH with a DUSP4 probe confirmed the colocalization of PITX1 and DUSP4 in mouse lung tissues and PSMCs (Fig. 7G, H). Furthermore, siRNAs were designed to knock down DUSP4, which was confirmed by Western blot analysis was performed to determine the knockdown efficiency (Fig. 7I). PITX1 overexpression prevented hypoxia-induced LDH release, whereas this preventative effect was abolished by DUSP4 knockdown (Fig. 7J). Electron microscopy revealed nuclear condensation and cell membrane rupture under hypoxic conditions, but these phenomena were inhibited by PITX1 overexpression. However, simultaneous knockdown of DUSP4 led to nuclear fragmentation and cytoplasmic vacuolization, with visible pores and rupture of the cell membrane (Fig. 7K). Consistent changes in the levels of pyroptosis-related proteins were observed (Fig. 7L). Overall, we conclude that PITX1 regulates pyroptosis in PSMCs through DUSP4.

Discussion

SEs can regulate the transcription of key genes to mediate the progression of many diseases. However, there are still relatively few studies on SEs in PAH. The present study has three major novel findings. First, the expression

of PITX1 was upregulated in SuHx PAH model mice and mice with hypoxic PH as well as in cultured PSMCs exposed to hypoxic conditions. Second, PITX1 coordinated with SEs to regulate the expression of DUSP4. Third, overexpression of PITX1/DUSP4 protected against pulmonary vascular remodeling, whereas their knockdown would aggravate PSMCs pyroptosis and promote pulmonary vascular remodeling. Therefore, DUSP4 expression is associated with PSMCs pyroptosis during PAH and that DUSP4 expression is regulated cooperatively by the SE and PITX1.

Pyroptosis was referred to be an inflammatory and programmed cell death mode first discovered in 1992 by Zychlinsky et al., and it was primarily involved three signaling pathways: the classical Caspase-1 pathway, the non-classical Caspase-4/5/11 pathway, and the Caspase-3/8-mediated pathway [32]. The pyroptotic cells exhibit entirely different morphological and biochemical characteristics compared with those of apoptotic, autophagic, and necrotic cells. Pyroptosis is an inflammatory necrosis caused by the activation of Caspase-1 that results in the formation of pores in the cell membrane and destruction of its integrity, in turn resulting in the release of cellular contents and increased permeability. As a new mode of programmed death, pyroptosis has been highly concerned in cancers, cardiovascular diseases, infections, and respiratory diseases [33–36]. Pyroptosis is closely related to the pathological process of tumors. Research has shown that Furthermore, pyroptosis plays a bidirectional role in tumors. On the one hand, pyroptosis reveals antitumor properties that can inhibit tumor cell growth. For instance, NLRP3 inflammasome could prevent the development of colon cancer [37], similar to AIM2 inflammasome in nasopharyngeal carcinoma [38]. Therefore, the formation of inflammasomes has a significant inhibitory effect on tumor progression. On the other hand, inflammatory components are produced during pyroptosis to activate proinflammatory cytokines,

(See figure on next page.)

Fig. 5 Inhibition of vascular remodeling and pyroptosis in hypoxic PH and SuHx PAH mice by upregulating the expression of DUSP4. **A, B** Immunofluorescence (IF) colocalization and fluorescence intensity of DUSP4 (red) and α SMA (green), with nuclei counterstained with DAPI (blue). Scale bar: 50 μ m. **C, E** Western blot: Representative images and statistical analysis of the gradient expression of DUSP4 in lung tissues and mPSMCs from mice subjected to hypoxia for 21 days. **F** Establishment of mouse models of hypoxic (10% O₂) PH and SuHx PAH, with DUSP4 knocked down via infection with AAV5 carrying shRNA. **G, N** Western blot: Representative images of the efficiency of DUSP4 knockdown in the SuHx PAH and hypoxic PH groups. **H, O** Immunofluorescence staining: Knockdown of DUSP4 and statistical analysis in the SuHx PAH and hypoxic PH groups. Scale bar: 50 μ m. **I, P** Representative echocardiograms (left) as well as statistical analysis of PAAT (right 1) and PAVTI (right 2), as measured by echocardiography. **J, Q** Statistical analysis of the right ventricular pressure and right ventricular hypertrophy index. **K, L, R, S** Representative images of H&E and Masson's trichrome staining in the lung tissue of the modeled mice. Scale bar: 50 μ m. (M, T) Western blot: Representative images as well as statistical data of NLRP3, ASC, GSDMD-N and IL-1 β levels. *Nor* normoxic, *Hyp* hypoxic, *NC* noncoding nucleotides, *shDUSP4* shRNADUSP4, *PAAT* pulmonary artery acceleration time, *PAVTI* pulmonary artery velocity time integral. All values are presented as means \pm SEMs (* p < 0.05, ** p < 0.01, and *** p < 0.001; $n \geq 3$)

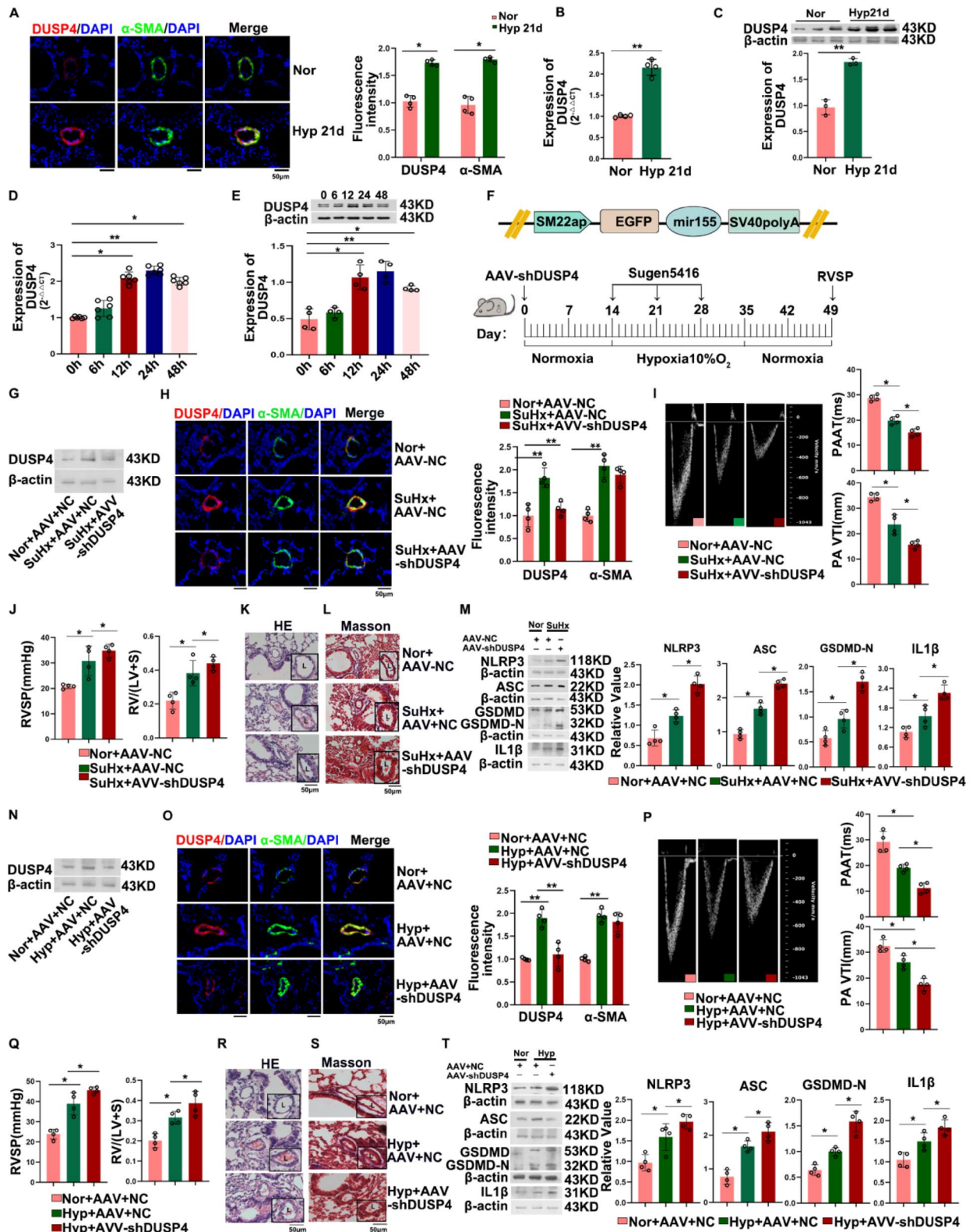


Fig. 5 (See legend on previous page.)

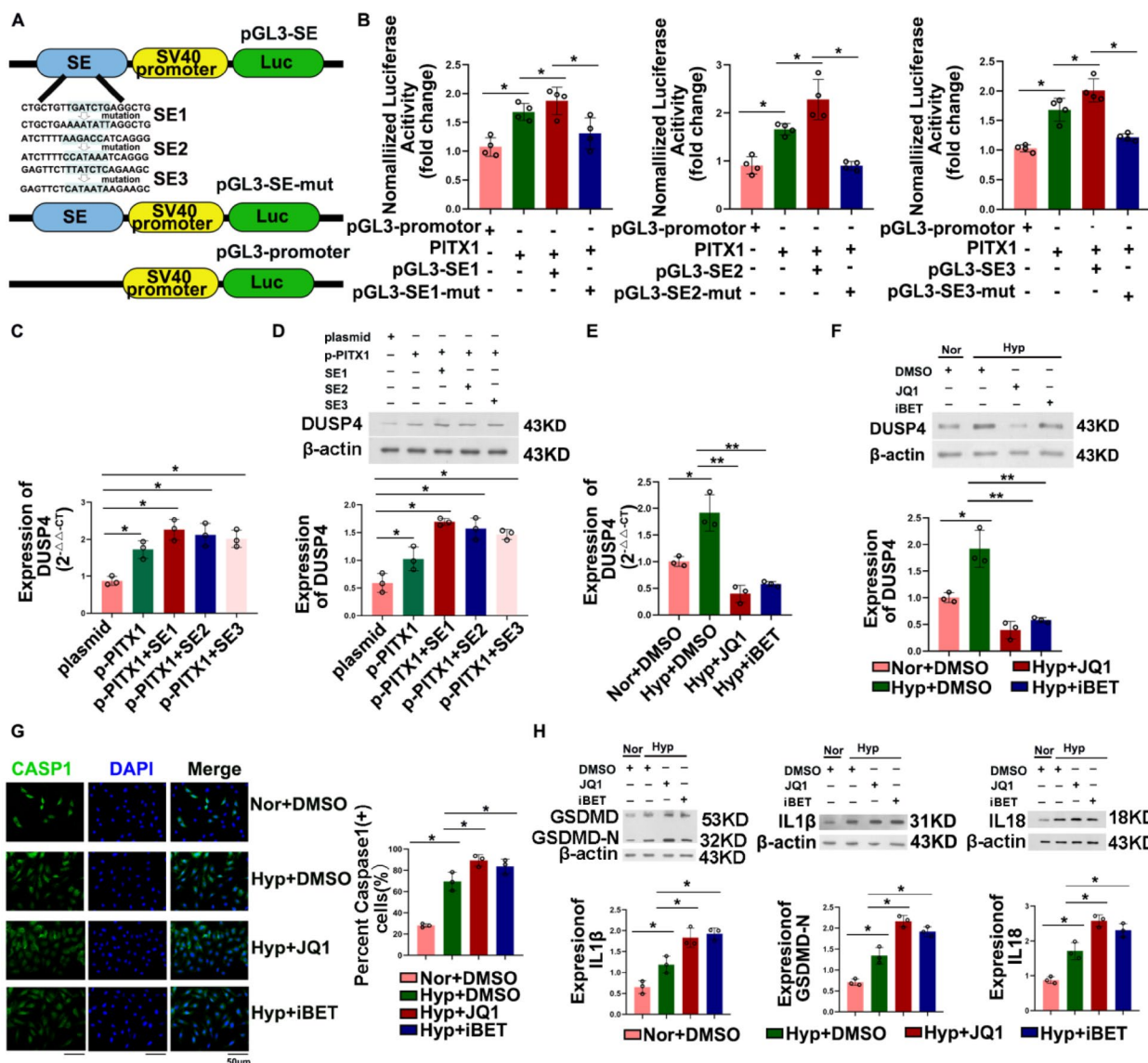


Fig. 6 Modulation of pyroptosis by influencing DUSP4 through its SE. **A, B** Construction of the dual-luciferase plasmid as well as statistical analysis of luciferase activity in mPASCs cotransfected with PITX1 plasmid and three segments of SE-DUSP4 or corresponding mutants for 24 h. **C, E** RT-qPCR: Changes in the transcript level of DUSP4 in mPASCs at the 24-h time point under hypoxic conditions after transfection with PITX1 plasmid and three segments of SE-DUSP4 after the addition of inhibitors JQ1 and iBET. **D, F** Western blot: Representative images as well as statistical data of the protein expression of DUSP4 in mPASCs at the 24-h time point under hypoxic conditions after transfection with PITX1 plasmid and three segments of SE-DUSP4 after the addition of inhibitors JQ1 and iBET. **G** Representative images and statistical data of positive CASP1 staining. Scale bar: 50 μm. **H** Western blot: Representative images as well as statistical analysis of the protein levels of GSDMD-N, IL-1β and IL-18. *Nor* normoxic, *Hyp* hypoxic. All values are presented as means ± SEMs (**p* < 0.05, and ***p* < 0.01; *n* ≥ 3)

promote the formation of the tumor microenvironment, and increase tumor growth [39, 40].

At present, the functions of pyroptosis during the process of PAH have been revealed by many studies. Additionally, multiple molecular mechanisms were gradually clarified with the continuous development of PAH. For instance, RPS4X could inhibit the pyroptosis based on the regulation of the glycosylation of

HSC70 [41]; Glioma-associated oncogene family zinc finger 1 promotes PASC pyroptosis through ASC [42]; SE-regulated CircLrch3 could form an R-loop with the host gene Lrch3, which regulated the pyroptosis in PASCs [10]; Cathepsin L induced the pyroptosis in PAECs by degrading Bmpr2 [43]; Caspase-4/11 modulated the TNF-α-induced pyroptosis within human PAECs, which showed effects on the pulmonary

vascular dysfunction and accelerated the progression of PAH [21, 44]. Moreover, the circ-Calm4/miR-124-3p/Pdcd6 axis showed significant importance within the hypoxia-induced pyroptosis of PASMCs [45], while dihydromyricetin (DMY) exhibited therapeutic effects on PAH by regulating the chemokine CKLF1/CC5 [46]. All the findings mentioned above could provide new insights into the deep understanding of the pathological mechanisms of PAH and the further exploration of the potential therapeutic targets. Nevertheless, the specific mechanisms remained to be clarified in highly malignant PAH due to the complex pathological process of the pyroptosis.

The SE region was characterized by DNA hypomethylation, open chromatin structures and transcription factor binding sites. It was found in previous research that the NLRP3 gene exhibited SE-related characteristics in monocytes and neutrophils, with low DNA methylation and hypersensitivity to DNase I. and the SE-related chromatin could up-regulate the expression of NLRP3. In addition, Caspase-1 and ASC genes were similarly featured by the DNA hypomethylation and large amounts of SE chromatin. Simultaneously, the NLRP3 gene expression was confirmed to be regulated by SE according to these results. Notably, Lysine methyltransferase 2D (KMT2D, also known as MLL4) was able to modify, regulate, and enhance the expression of subregion gene by catalyzing the methylation of histone, and it was involved in physiological processes such as development and cell differentiation. According to the existing studies, KMT2D could activate the GSDMD-mediated pyroptosis by affecting the SE-regulated RNA-induced silencing complex (RISC) and DNA methyltransferase expression [11], in tumor cells. Additionally, SE in nucleus pulposus cells (NP Cells) were confirmed to show repressive effects on the transcription of genes related to inflammatory cascades and extracellular matrix remodeling (e.g.,

IL1 β) [47]. It could be suggested by the above literature that the alterations during the SE process tended to indirectly regulate the expression of pyroptosis proteins through different pathways, which in turn influence the pyroptosis process. Additionally, this paper was based on the above foundation and aimed to add valid evidence for further exploration. Research has found that the hypoxia could up-regulate the expression of pyroptosis proteins Caspase-1, GSDMD-N-terminal, IL-18, and IL1 β in PASMCs, while SE inhibitors including JQ1 and iBET reduced the transcription level of DUSP4 by inhibiting its SE activity, thereby exacerbating the pyroptosis. Additionally, it could confirm the fact that the changes in SE activity indirectly affected the pyroptosis process based on the regulation of the target genes. However, the specific changes in SE activity that directly regulated the pyroptosis, alongside the deep mechanisms by which DUSP4 regulated the pyroptosis remained to be clarified in further studies. Overall, our research group would further explore the relationship between SE and the pyroptosis, and more attention would be paid to the clarification of the impacts and mechanisms of SE activity alterations on the expression of PAH-related pyroptosis genes. With these efforts, it was expected to provide a theoretical basis for the prevention and treatment of pyroptosis in PAH through the regulation of SE activity.

Jayaprakash et al. found that ARID1A could regulate DUSP4 expression via chromatin remodeling, further inhibiting endometrial cancer development through the MAPK pathway [48]. ChIP-seq analysis showed that compared with wild-type human endometrial epithelial cells, ARID1A-knockout human endometrial epithelial cells presented reduced enrichment of the active transcriptional histone marks H3K27ac and H3K9ac in the DUSP4 regulatory region, leading to significant downregulation of DUSP4 expression. However, their experimental results only confirmed the impact of ARID1A on DUSP4 enhancer, but not the SE-DUSP4.

(See figure on next page.)

Fig. 7 PITX1 modulating pulmonary vascular remodeling and pyroptosis through DUSP4. **A** Establishment of a hypoxic (10% O₂) mouse model with overexpression of PITX1 and knockdown of DUSP4 via AAV5. **B** Representative echocardiogram (left) as well as statistical analysis of PAAT (right 1) and PAVTI (right 2). **C** Statistical analysis of right ventricular pressure and right ventricular hypertrophy index. **D, E** Representative images of H&E and Masson's trichrome staining in the lung tissue of the modeled mice. Scale bar: 50 μ m. **F** Western blot: Representative images as well as statistical analysis of NLRP3, ASC, CASP1, GSDMD-N and IL-1 β levels. **G, H** Immunofluorescence staining of PITX1 (red) with an antibody and DUSP4 (green) with fluorescence in situ hybridization (FISH) probes to demonstrate their colocalization in the lung tissues and mPASMCs of mice. Nuclei were counterstained with DAPI (blue). Scale bars: 25 μ m, and 100 μ m. **I** Western blot: Representative image showing the interference efficiency of siDUSP4. **J** LDH assay: Determination of the number of dead mPASMCs by quantifying the amount of LDH released from the membrane of damaged cells. **K** SEM: Morphological observation of nuclear, cytoplasmic, and membrane integrity as well as pore formation following PITX1 overexpression combined with DUSP4 knockdown, compared with those under hypoxic conditions and with PITX1 overexpression alone. Scale bar: 5 μ m. **L** Western blot: Representative images as well as statistical data of CASP1, GSDMD-N, IL-1 β , and IL-18 levels. PAAT pulmonary artery acceleration time, PAVTI pulmonary artery velocity time integral, Nor normoxic, Hyp hypoxic, NC noncoding nucleotides, shDUSP4 shRNADUSP4, AAV AAV5, adeno-associated virus 5. All values are presented as means \pm SEMs (* p < 0.05, and ** p < 0.01; $n \geq 3$)

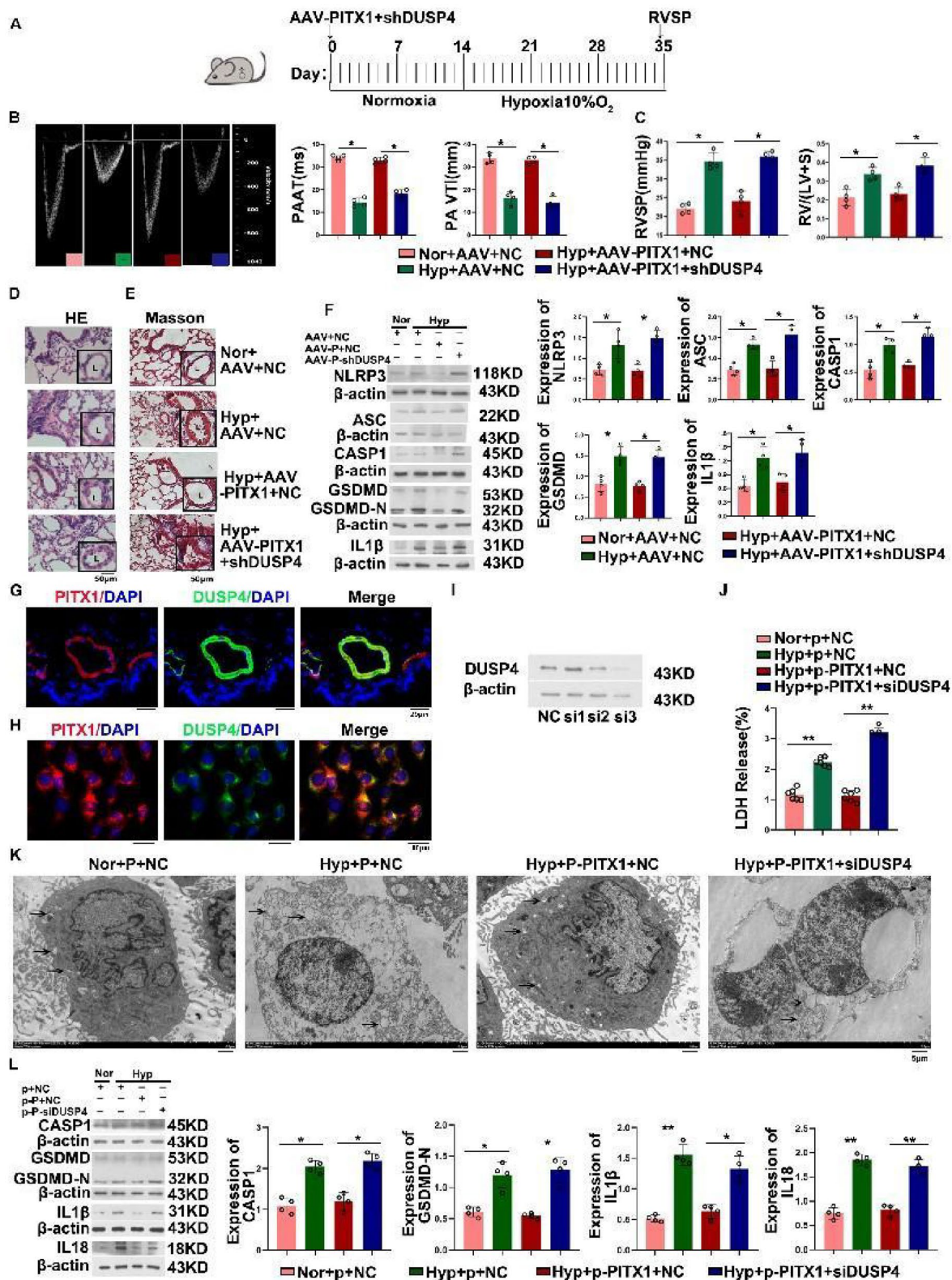


Fig. 7 (See legend on previous page.)

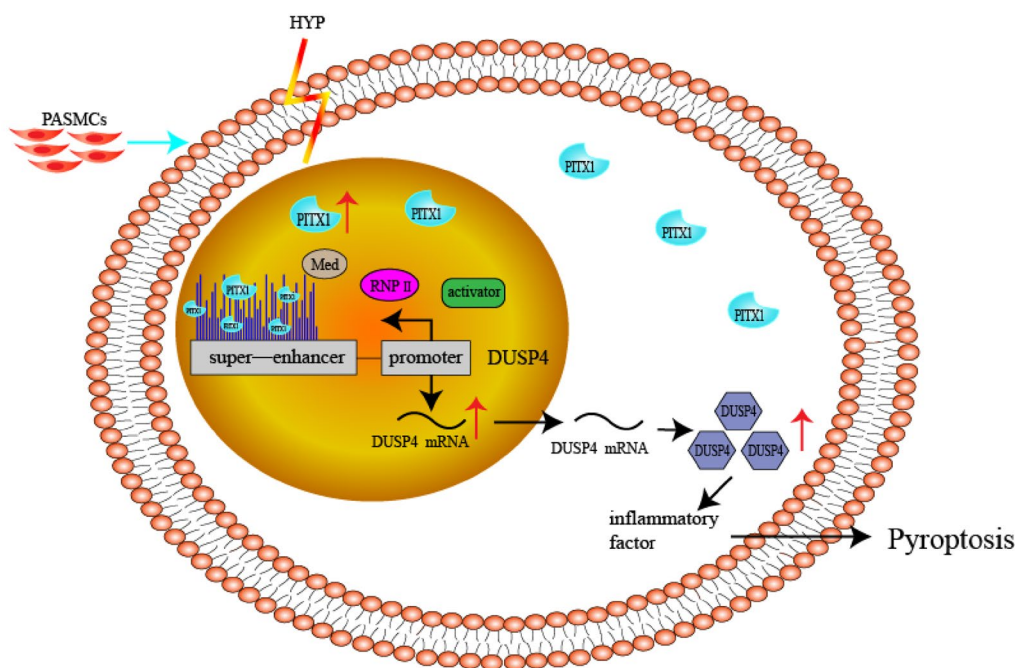


Fig. 8 Model of the regulation of pyroptosis by PITX1 via DUSP4 in PAH. In this model, PITX1 promotes the expression of DUSP4 by binding to SE-DUSP4 and affects pyroptosis in pulmonary arterial smooth muscle cells and pulmonary vascular remodeling. PITX1 = Paired-like homeodomain transcription factor 1; DUSP4 = Dual-specificity phosphatase 4; and RNP II = RNA polymerase II

Notably in our study, the SE sequences involved in the transcriptional regulation of DUSP4 were identified and distinguished via ChIP-seq with an anti-H3K27ac antibody. The molecular mechanism of the SE in DUSP4 transcriptional regulation was fully revealed via a dual-luciferase reporter assay (Figs. 4 and 6).

Abnormal DUSP4 expression, showing relationship with the regulation of various transcription factors, has been implicated in the pathogenesis of many diseases. For example, CTCF, STAT3, YY1 and other transcription factors can regulate the transcriptional events of DUSP4 in a promoter-specific manner [49]. Moreover, DUSP4 transcription can also be regulated by other transcription factors, e.g., p53 [50], E2F1 [51], and ETS1 [52]. Moreover, the above findings confirmed that the abnormal expression of DUSP4 in the context of disease is related to these transcription factors. Via ALGGEN-PROMO, AnimalTFDB, JASPAR and other databases, we predicted that the transcription factor PITX1 has binding sites in both the promoter and SE sequences of DUSP4. ChIP-qPCR analysis and dual-luciferase reporter assays further confirmed the effect of PITX1 on DUSP4 transcriptional activity. Therefore, PITX1 can be regarded as a novel transcription factor to regulate DUSP4 expression.

Furthermore, DUSP4 can affect disease course by inhibiting the activation of ERK, JNK, and p38-MAPK

signaling pathways. For example, DUSP4 promoter methylation and low DUSP4 expression led to inactivated Ras/MAPK pathway, promoting the proliferation and anticancer drug resistance of breast cancer cells [53]. DUSP4 could also regulate ERK signaling to prevent acute lung injury in pulmonary microvascular endothelial cells [27]. Besides, DUSP4 deficiency could mediate lenvatinib resistance by activating the MAPK/ERK signaling pathway [54]. More importantly, our previous studies confirmed that the ERK, JNK and p38-MAPK signaling pathways play important regulatory roles in the proliferation of PASMCS and pulmonary artery endothelial cells (PAECs) and in pulmonary vascular remodeling [55, 56]. MAPK also plays a key role in the new pathological process of pyroptosis. In addition, JNK in the MAPK signaling pathway would support inflammasome-mediated IL-1 β secretion and pyroptosis in human macrophages [57].

According to prior research, MAPK signaling is a contributor of pyroptosis and PAH [21, 44]. Therefore, the present study continued to speculate that DUSP4 might exert an inhibitory role on the pyroptosis of PASMCS by inactivating MAPK signaling pathway. We carried out AAV5-mediated shRNA transduction to reduce DUSP4 expression in both the hypoxic PH model and SuHx PAH model and found that DUSP4 expression decreased; as well as increased RVSP, the right ventricular hypertrophy

index, the PAAT/PAVTI ratio and pulmonary vascular remodeling, and pulmonary vascular cell pyroptosis. However, in view of the preliminary research, further investigation is needed to decipher the mechanism by which DUSP4 affects pulmonary vascular cell pyroptosis through the MAPK pathway.

PITX1 is a highly conserved homeobox gene with varied expressions and functions that has been extensively studied in various tumors. PITX1 has been reported to be a tumor suppressor whose expression is reduced in esophageal squamous cell carcinoma, rectal cancer, and melanoma [58–60]. However, the expression of PITX1 was upregulated in breast cancer and lung cancer, which was associated with poor prognosis [61, 62]. This difference may be largely attributed to differences in the tumor microenvironment or cell lines. The results of the present study confirmed that the expression of PITX1 was upregulated under hypoxic conditions. Reduction of PITX1 expression in vitro could increase pyroptosis in hypoxic PSMCs, whereas exogenous PITX1 supplementation reversed hypoxia-induced increase in the pyroptosis of PSMCs. Moreover, the overexpression of PITX1 via AAV5 alleviated the increase in right ventricular pressure, the right ventricular hypertrophy index and PSMCs pyroptosis, restored the PAAT/PAVTI ratio; and reduced the degree of pulmonary vascular remodeling in both SuHx PAH and hypoxic PH mice. Numerous factors are released in response to external stimuli in vivo. Studies in myocardial diseases have shown the activation or upregulation of some protective factors in the myocardium in response to external stimuli. The expression of Heat shock factor 1 (HSF1), a transcription factor, was upregulated in palmitic acid-induced myocardial injury, and overexpression of HSF1 ameliorated myocardial injury [63]. In addition, the expression of DNA methyltransferase3b (DNMT3b), a protective factor for hypoxia-induced pulmonary vascular remodeling, was increased under hypoxic conditions but not under normoxic conditions, which retarded the development of PAH [64]. On the basis of the above theoretical and experimental results, we believe that the upregulation of PITX1 may be a protective response in pulmonary vessels stimulated by hypoxia.

So far, there is still insufficient data on SEs in PAH, despite existing evidence to support the involvement of SEs in pulmonary vascular remodeling during PH by affecting the pyroptosis pathway. Innovatively, the present study discovers that the epigenetic regulation of DUSP4 by PITX1 and the SE may interfere with the pyroptosis of PSMCs and pulmonary vascular remodeling, which may provide favorable reference for the prevention and treatment of PAH.

Conclusions

In summary, PITX1 can promote DUSP4 expression by binding to the promoter and SE of DUSP4, which may reduce the pyroptosis of PSMCs during hypoxia, eventually affecting vascular remodeling and regulating pyroptosis-related pathology through the PITX1-SE-DUSP4 axis in PAH (Fig. 8).

Abbreviations

PH	Pulmonary hypertension
PAH	Pulmonary arterial hypertension
SE	Super-enhancer
PASMCs	Pulmonary artery smooth muscle cells
NLRP3	NOD-like receptor protein 3
ASC	Apoptosis-associated speck-like protein containing a caspase activation and recruitment domain
CASP1	Recombinant caspase 1
GSDMD	Gasdermin D
IL18/1 β	Interleukin 18/1 β
FISH	Fluorescence in situ hybridization
RT-qPCR	Reverse transcription-quantitative polymerase chain reaction
ChIP-qPCR	Chromatin immunoprecipitation-quantitative polymerase chain reaction
H&E	Hematoxylin and eosin staining
JQ1	BET bromodomain inhibitor
iBET	GSK1210151A
iBET151	BET bromodomain inhibitor

Supplementary Information

The online version contains supplementary material available at <https://doi.org/10.1186/s12931-025-03222-9>.

Supplementary material 1. (A) Identification of 1,585 upregulated genes in hypoxic PSMCs via heatmap analysis and gene set enrichment analysis. (B) Enrichment of H3K27ac in 50 genes by H3K27ac ChIP-seq. (C) Venn diagram of 14 genes with upregulated expression and enrichment of H3K27ac under hypoxic conditions.

Acknowledgements

This work was supported by the National Natural Science Foundation of China (32171122 to Y.X.; 82241006; 32071120 to X. Zheng); Heilongjiang Natural Science Foundation Joint Guidance Project (LH2021H019 to Y.X.); The Fundamental Research Funds for the Provincial Universities (JFYWH202002 to Y.X.); Construction Project of Scientific Research and Innovation Team of Harbin Medical University-Daqing (HD-CXTD-202001).

Author contributions

JYZ, YYS, YX, and XDZ designed and supervised this study; JYZ, XYS, and XW performed the cell experiments; SYL,BSZ,and CZ performed the animal experiments;JYZ,BSZ,and YYT prepared pathological sections; YX,XRW,and JQ performed the statistical analysis; JYZ, YX and XDZ wrote the manuscript; all authors contributed to manuscript revision. All authors read and approved the final manuscript.

Funding

This work was supported by the National Natural Science Foundation of China (No.32171122 to Y.X.; No.82241006; No.32071120 to X. Zheng); Heilongjiang Natural Science Foundation Joint Guidance Project (No.LH2021H019 to Y.X.); The Fundamental Research Funds for the Provincial Universities (No. JFYWH202002 to Y.X.); as well as Construction Project of Scientific Research and Innovation Team of Harbin Medical University-Daqing (No.HD-CXTD-202001).

Data availability

No datasets were generated or analysed during the current study.

Declarations

Ethics approval and consent to participate

Animal care and use were performed in accordance with the National Institutes of Health Guide for the Care and Use of Laboratory Animals (National Institutes of Health Publication 85-23, revised 1996); and all animal protocols were approved by the Ethical Committee of Harbin Medical University (Daqing) (No.HMUDQ20240627001).

Consent for publication

Not applicable.

Competing interests

The authors declare no competing interests.

Author details

¹Department of Pharmacology, Harbin Medical University-Daqing, Daqing 163319, Heilongjiang, People's Republic of China. ²College of Pharmacy, Harbin Medical University, Harbin 150081, Heilongjiang, People's Republic of China. ³Department of Literature Retrieval, Harbin Medical University, Daqing 150081, Heilongjiang, People's Republic of China. ⁴Department of Pathology, Gaozhou People's Hospital, Gaozhou 525299, Guangdong, People's Republic of China. ⁵Department of Pathology, Harbin Medical University-Daqing, Daqing 163319, Heilongjiang, People's Republic of China. ⁶Department of Medical Genetics, Harbin Medical University-Daqing, Daqing 163319, Heilongjiang, People's Republic of China.

Received: 8 October 2024 Accepted: 5 April 2025

Published online: 16 April 2025

References

- Xing Y, Zheng X, Fu Y, Qi J, Li M, Ma M, Wang S, Li S, Zhu D. Long noncoding RNA-maternally expressed gene 3 contributes to hypoxic pulmonary hypertension. *Mol Ther*. 2019;27(12):2166–81. <https://doi.org/10.1016/j.jymthe.2019.07.022>.
- Simonneau G, Montani D, Celermajer DS, Denton CP, Gatzoulis MA, Krowka M, Williams PG, Souza R. Haemodynamic definitions and updated clinical classification of pulmonary hypertension. *Eur Respir J*. 2019. <https://doi.org/10.1183/13993003.01913-2018>.
- Dai J, Zhou Q, Chen J, Rexius-Hall ML, Rehman J, Zhou G. Alpha-enolase regulates the malignant phenotype of pulmonary artery smooth muscle cells via the AMPK-Akt pathway. *Nat Commun*. 2018. <https://doi.org/10.1038/s41467-018-06376-x>.
- Hassoun PM, Taichman DB. Pulmonary arterial hypertension. *N Engl J Med*. 2021;385(25):2361–76. <https://doi.org/10.1056/NEJMr2000348>.
- Wang X, Li Q, He S, Bai J, Ma C, Zhang L, Guan X, Yuan H, Li Y, Zhu X, Mei J, Gao F, Zhu D. LncRNA FENDRR with m6A RNA methylation regulates hypoxia-induced pulmonary artery endothelial cell pyroptosis by mediating DRP1 DNA methylation. *Mol Med*. 2022. <https://doi.org/10.1186/s10020-022-00551-z>.
- Blayney JW, Francis H, Rampasekova A, Camellato B, Mitchell L, Stolper R, Cornell L, Babbs C, Boeke JD, Higgs DR, Kassouf M. Super-enhancers include classical enhancers and facilitators to fully activate gene expression. *Cell*. 2023;186(26):5826–5839.e5818. <https://doi.org/10.1016/j.cell.2023.11.030>.
- Whyte Warren A, Orlando David A, Hnisz D, Abraham Brian J, Lin Charles Y, Kagey Michael H, Rahl Peter B, Lee Tong I, Young RA. Master transcription factors and mediator establish super-enhancers at key cell identity genes. *Cell*. 2013;153(2):307–19. <https://doi.org/10.1016/j.cell.2013.03.035>.
- Chen H, Liang H. A high-resolution map of human enhancer RNA loci characterizes super-enhancer activities in cancer. *Cancer Cell*. 2020;38(5):701–15. <https://doi.org/10.1016/j.ccell.2020.08.020>.
- Wang M, Chen Q, Wang S, Xie H, Liu J, Huang R, Xiang Y, Jiang Y, Tian D, Bian E. Super-enhancers complexes zoom in transcription in cancer. *J Exp Clin Cancer Res*. 2023. <https://doi.org/10.1186/s13046-023-02763-5>.
- Liu H, Jiang Y, Shi R, Hao Y, Li M, Bai J, Wang H, Guan X, Song X, Ma C, Zhang L, Zhao X, Zheng X, Zhu D. Super enhancer-associated circRNA-circLrhc3 regulates hypoxia-induced pulmonary arterial smooth muscle cells pyroptosis by formation of R-loop with host gene. *Int J Biol Macromol*. 2024. <https://doi.org/10.1016/j.jbiomac.2024.130853>.
- Ning H, Huang S, Lei Y, Zhi R, Yan H, Jin J, Hu Z, Guo K, Liu J, Yang J, Liu Z, Ba Y, Gao X, Hu D. Enhancer decommissioning by MLL4 ablation elicits dsRNA-interferon signaling and GSDMD-mediated pyroptosis to potentiate anti-tumor immunity. *Nat Commun*. 2022. <https://doi.org/10.1038/s41467-022-34253-1>.
- Son S-H, Son Y-E, Cho H-J, Chen W, Lee M-K, Kim L-H, Han D-M, Park H-S. Homeobox proteins are essential for fungal differentiation and secondary metabolism in *Aspergillus nidulans*. *Sci Rep*. 2020. <https://doi.org/10.1038/s41598-020-63300-4>.
- Vonk PJ, Ohm RA. The role of homeodomain transcription factors in fungal development. *Fungal Biol Rev*. 2018;32(4):219–30. <https://doi.org/10.1016/j.fbr.2018.04.002>.
- Kragestein BK, Spielmann M, Paliou C, Heinrich V, Schöpflin R, Esposito A, Annunziatella C, Bianco S, Chiariello AM, Jerković I, Harabula I, Guckelberger P, Pechstein M, Wittler L, Chan W-L, Franke M, Lupiáñez DG, Kraft K, Timmermann B, Vingron M, Visel A, Nicodemi M, Mundlos S, Andrey G. Dynamic 3D chromatin architecture contributes to enhancer specificity and limb morphogenesis. *Nat Genet*. 2018;50(10):1463–73. <https://doi.org/10.1038/s41588-018-0221-x>.
- Liu DX, Lobie PE. Transcriptional activation of p53 by Pitx1. *Cell Death Differ*. 2007;14(11):1893–907. <https://doi.org/10.1038/sj.cdd.4402209>.
- Ohira T, Nakagawa S, Takeshita J, Aburatani H, Kugoh H. PITX1 inhibits the growth and proliferation of melanoma cells through regulation of SOX family genes. *Sci Rep*. 2021. <https://doi.org/10.1038/s41598-021-97791-6>.
- Sastre-Perona A, Hoang-Phou S, Leitner M-C, Okuniewska M, Meehan S, Schober M. De novo PITX1 expression controls Bi-stable transcriptional circuits to govern self-renewal and differentiation in squamous cell carcinoma. *Cell Stem Cell*. 2019;24(3):390–404.e398. <https://doi.org/10.1016/j.stem.2019.01.003>.
- Mudie S, Bandarra D, Batie M, Biddlestone J, Moniz S, Ortmann B, Shmakova A, Rocha S. PITX1, a specificity determinant in the HIF-1 α -mediated transcriptional response to hypoxia. *Cell Cycle*. 2015;13(24):3878–91. <https://doi.org/10.4161/15384101.2014.972889>.
- Xing Y, Qi J, Cheng X, Song X, Zhang J, Li S, Zhao X, Gong T, Yang J, Zhao C, Xin W, Zhu D, Zheng X. Circ-myl8 promotes pulmonary hypertension by recruiting kat7 to govern hypoxia-inducible factor-1 α expression. *J Am Heart Assoc*. 2023. <https://doi.org/10.1161/jaha.122.028299>.
- Caunt CJ, Keyse SM. Dual-specificity MAP kinase phosphatases (MKPs). *FEBS J*. 2012;280(2):489–504. <https://doi.org/10.1111/j.1742-4658.2012.08716.x>.
- Wu Z, Zhou G, Wang H, Yao P. Inhibition of KIF23 alleviates IPAH by targeting pyroptosis and proliferation of PAMSCs. *Int J Mol Sci*. 2022. <https://doi.org/10.3390/ijms23084436>.
- Yu X, Li T, Liu X, Yu H, Hao Z, Chen Y, Zhang C, Liu Y, Li Q, Mao M, Zhu D. Modulation of pulmonary vascular remodeling in hypoxia: role of 15-LOX-2/15-HETE-MAPKs pathway. *Cell Physiol Biochem*. 2015;35(6):2079–97. <https://doi.org/10.1159/000374015>.
- Gupta A, Towers C, Willenbrock F, Brant R, Hodgson DR, Sharpe A, Smith P, Cutts A, Schuh A, Asher R, Myers K, Love S, Collins L, Wise A, Middleton MR, Macaulay VM. Dual-specificity protein phosphatase DUSP4 regulates response to MEK inhibition in BRAF wild-type melanoma. *Br J Cancer*. 2019;122(4):506–16. <https://doi.org/10.1038/s41416-019-0673-5>.
- Chen M, Zhang J, Berger AH, DiIolombi MS, Ng C, Fung J, Bronson RT, Castillo-Martin M, Thin TH, Cordon-Cardo C, Plevin R, Pandolfi PP. Compound haploinsufficiency of Dok2 and Dusp4 promotes lung tumorigenesis. *J Clin Invest*. 2018;129(1):215–22. <https://doi.org/10.1172/jci99699>.
- Mandal J, Yu Z-C, Shih I-M, Wang T-L. ARID1A loss activates MAPK signaling via DUSP4 downregulation. *J Biomed Sci*. 2023. <https://doi.org/10.1186/s12929-023-00985-5>.
- Barajas-Espinosa A, Basye A, Angelos M, Chen CA. Modulation of p38 MAPK by DUSP4 is important in regulating cardiovascular function under oxidative stress. *Free Radical Biology and Medicine*. 2015;89:170–81. <https://doi.org/10.1016/j.freeradbiomed.2014.06.016>.
- Lu Z, Feng H, Shen X, He R, Meng H, Lin W, Geng Q. MiR-122-5p protects against acute lung injury via regulation of DUSP4/ERK signaling in pulmonary microvascular endothelial cells. *Life Sci*. 2020. <https://doi.org/10.1016/j.lfs.2020.117851>.

28. Zhou L, Yao N, Yang L, Liu K, Qiao Y, Huang C, Du R, Yeung YT, Liu W, Cheng D, Dong Z, Li X. DUSP4 promotes esophageal squamous cell carcinoma progression by dephosphorylating HSP90 β . *Cell Rep*. 2023. <https://doi.org/10.1016/j.celrep.2023.112445>.
29. Xu W, Chen B, Ke D, Chen X. DUSP4 directly deubiquitinates and stabilizes Smad4 protein, promoting proliferation and metastasis of colorectal cancer cells. *Aging*. 2020. <https://doi.org/10.18632/aging.103823>.
30. Yang C, Zang Y, Wu S, Zhou Q, Ou Y, Ding Q, Wang H, Xiong Z. Silencing circFTO inhibits malignant phenotype through modulating DUSP4 expression in clear cell renal cell carcinoma. *Cell Death Discov*. 2022. <https://doi.org/10.1038/s41420-022-01138-7>.
31. Wu H, Fu Q, Li Z, Wei H, Qin S. Inhibition of microRNA-122 alleviates pyroptosis by targeting dual-specificity phosphatase 4 in myocardial ischemia/reperfusion injury. *Heliyon*. 2023. <https://doi.org/10.1016/j.heliyon.2023.e18238>.
32. Yu P, Zhang X, Liu N, Tang L, Peng C, Chen X. Pyroptosis: mechanisms and diseases. *Signal Transduct Target Ther*. 2021. <https://doi.org/10.1038/s41392-021-00507-5>.
33. Fang Y, Tian S, Pan Y, Li W, Wang Q, Tang Y, Yu T, Wu X, Shi Y, Ma P, Shu Y. Pyroptosis: a new frontier in cancer. *Biomed Pharmacother*. 2020. <https://doi.org/10.1016/j.biopha.2019.109595>.
34. Feng Y, Li M, Yangzhong X, Zhang X, Zu A, Hou Y, Li L, Sun S. Pyroptosis in inflammation-related respiratory disease. *J Physiol Biochem*. 2022;78(4):721–37. <https://doi.org/10.1007/s13105-022-00909-1>.
35. LaRock DL, Johnson AF, Wilde S, Sands JS, Monteiro MP, LaRock CN. Group A Streptococcus induces GSDMA-dependent pyroptosis in keratinocytes. *Nature*. 2022;605(7910):527–31. <https://doi.org/10.1038/s41586-022-04717-x>.
36. Yarovinsky TO, Su M, Chen C, Xiang Y, Tang WH, Hwa J. Pyroptosis in cardiovascular diseases: pumping gasdermin on the fire. *Semin Immunol*. 2023. <https://doi.org/10.1016/j.smim.2023.101809>.
37. Dupaul-Chicoine J, Arabzadeh A, Dagenais M, Douglas T, Champagne C, Morizot A, Rodrigue-Gervais Ian G, Breton V, Colpitts Sara L, Beauchemin N, Saleh M. The Nlrp3 inflammasome suppresses colorectal cancer metastatic growth in the liver by promoting natural killer cell tumoricidal activity. *Immunity*. 2015;43(4):751–63. <https://doi.org/10.1016/j.immuni.2015.08.013>.
38. Di M, Miao J, Pan Q, Wu Z, Chen B, Wang M, Zhao J, Huang H, Bai J, Wang Q, Tang Y, Li Y, He J, Xiang T, Weng D, Wang L, Xia J, Zhao C. OTUD4-mediated GSDME deubiquitination enhances radiosensitivity in nasopharyngeal carcinoma by inducing pyroptosis. *J Exp Clin Cancer Res*. 2022. <https://doi.org/10.1186/s13046-022-02533-9>.
39. Ershaid N, Sharon Y, Doron H, Raz Y, Shani O, Cohen N, Monteran L, Leider-Trejo L, Ben-Shmuel A, Yassin M, Gerlic M, Ben-Baruch A, Pasmank-Chor M, Apte R, Erez N. NLRP3 inflammasome in fibroblasts links tissue damage with inflammation in breast cancer progression and metastasis. *Nat Commun*. 2019. <https://doi.org/10.1038/s41467-019-12370-8>.
40. Kaplanov I, Carmi Y, Kornetsky R, Shemesh A, Shurin GV, Shurin MR, Dinarello CA, Voronov E, Apte RN. Blocking IL-1 β reverses the immunosuppression in mouse breast cancer and synergizes with anti-PD-1 for tumor abrogation. *Proc Natl Acad Sci*. 2018;116(4):1361–9. <https://doi.org/10.1073/pnas.1812266115>.
41. Li Y, Zhang J, Sun H, Yu X, Chen Y, Ma C, Zheng X, Zhang L, Zhao X, Jiang Y, Xin W, Wang S, Hu J, Wang M, Zhu D. RPS4XL encoded by Inc-Rps4l inhibits hypoxia-induced pyroptosis by binding HSC70 glycosylation site. *Mol Ther Nucleic Acids*. 2022;28:920–34. <https://doi.org/10.1016/j.omtn.2022.05.033>.
42. He S, Ma C, Zhang L, Bai J, Wang X, Zheng X, Zhang J, Xin W, Li Y, Jiang Y, Wang S, Zhu D. GLI1-mediated pulmonary artery smooth muscle cell pyroptosis contributes to hypoxia-induced pulmonary hypertension. *Am J Physiol Lung Cell Mol Physiol*. 2020; 318(3):L472–82. <https://doi.org/10.1152/ajplung.00405.2019>.
43. Peng Z, Luo XY, Li X, Li Y, Wu Y, Tian Y, Pan B, Petrovic A, Kosanovic D, Schermuly RT, Ruppert C, Gunther A, Zhang Z, Qiu C, Li Y, Pu J, Li X, Chen AF. Cathepsin L promotes pulmonary hypertension via BMPR2/GSDME-mediated pyroptosis. *Hypertension*. 2024;81(12):2430–43. <https://doi.org/10.1161/HYPERTENSIONAHA.124.22903>.
44. Wu Y, Pan B, Zhang Z, Li X, Leng Y, Ji Y, Sun K, Chen AF. Caspase-4/11-mediated pulmonary artery endothelial cell pyroptosis contributes to pulmonary arterial hypertension. *Hypertension*. 2022;79(3):536–48. <https://doi.org/10.1161/HYPERTENSIONAHA.121.17868>.
45. Jiang Y, Liu H, Yu H, Zhou Y, Zhang J, Xin W, Li Y, He S, Ma C, Zheng X, Zhang L, Zhao X, Wu B, Jiang C, Zhu D. Circular RNA Calm4 regulates hypoxia-induced pulmonary arterial smooth muscle cells pyroptosis via the Circ-Calm4/miR-124-3p/PDCD6 axis. *Arterioscler Thromb Vasc Biol*. 2021;41(5):1675–93. <https://doi.org/10.1161/atvbaha.120.315525>.
46. Yan Q, Li P, Liu S, Sun Y, Chen C, Long J, Lin Y, Liang J, Wang H, Zhang L, Wang H, Wang H, Yang S, Lin M, Liu X, Yao J, Tian Z, Chen N, Yang Y, Ai Q. Dihydropyridinone treats pulmonary hypertension by modulating CKLF1/CCR5 axis-induced pulmonary vascular cell pyroptosis. *Biomed Pharmacother*. 2024. <https://doi.org/10.1016/j.biopha.2024.117614>.
47. Li G, Kang Y, Feng X, Wang G, Yuan Y, Li Z, Du L, Xu B. Dynamic changes of enhancer and super enhancer landscape in degenerated nucleus pulposus cells. *Life Sci Alliance*. 2023. <https://doi.org/10.26508/lsa.202201854>.
48. Mandal J, Yu ZC, Shih IM, Wang T. ARID1A loss activates MAPK signaling via DUSP4 downregulation. *J Biomed Sci*. 2023;30(11):94. <https://doi.org/10.1186/s12929-023-00985-5>.
49. Varela T, Conceição N, Laizé V, Cancela ML. Transcriptional regulation of human DUSP4 gene by cancer-related transcription factors. *J Cell Biochem*. 2021;122(10):1556–66. <https://doi.org/10.1002/jcb.30078>.
50. Yin R, Eger G, Sarri N, Rorsman C, Heldin C-H, Lennartsson J. Dual specificity phosphatase (DUSP)-4 is induced by platelet-derived growth factor -BB in an Erk1/2-, STAT3- and p53-dependent manner. *Biochem Biophys Res Commun*. 2019;519(3):469–74. <https://doi.org/10.1016/j.bbrc.2019.09.014>.
51. Wang J, Shen WH, Jin YJ, Brandt-Rauf PW, Yin Y. A molecular link between E2F-1 and the MAPK cascade. *J Biol Chem*. 2007;282(25):18521–31. <https://doi.org/10.1074/jbc.M610538200>.
52. Plotnik JP, Budka JA, Ferris MW, Hollenhorst PC. ETS1 is a genome-wide effector of RAS/ERK signaling in epithelial cells. *Nucleic Acids Res*. 2014;42(19):11928–40. <https://doi.org/10.1093/nar/gku929>.
53. Balko J, Schwarz L, Bhola N, Kurupi R, Owens P, Miller T, Gomez H, Cook R, Arteaga C. Activation of MAPK pathways due to DUSP4 loss promotes cancer stem cell-like phenotypes in basal-like breast cancer. *Cancer Res*. 2013;73(20):6346–58. <https://doi.org/10.1158/0008-5472.Can-13-1385>.
54. Huang S, Ma Z, Zhou Q, Wang A, Gong Y, Li Z, Wang S, Yan Q, Wang D, Hou B, Zhang C. Genome-wide CRISPR/Cas9 library screening identified that DUSP4 deficiency induces lenvatinib resistance in hepatocellular carcinoma. *Int J Biol Sci*. 2022;18(11):4357–71. <https://doi.org/10.7150/ijbs.69969>.
55. Ma C, Liu Y, Wang Y, Zhang C, Yao H, Ma J, Zhang L, Zhang D, Shen T, Zhu D. Hypoxia activates 15-PGDH and its metabolite 15-KETE to promote pulmonary artery endothelial cells proliferation via ERK1/2 signalling. *Br J Pharmacol*. 2014;171(14):3352–63. <https://doi.org/10.1111/bph.12594>.
56. Ma J, Zhang L, Han W, Shen T, Ma C, Liu Y, Nie X, Liu M, Ran Y, Zhu D. Activation of JNK/c-Jun is required for the proliferation, survival, and angiogenesis induced by EET in pulmonary artery endothelial cells. *J Lipid Res*. 2012;53(6):1093–105. <https://doi.org/10.1194/jlr.M024398>.
57. Bradfield CJ, Liang JJ, Ernst O, John SP, Sun J, Ganesan S, de Jesus AA, Bryant CE, Goldbach-Mansky R, Fraser IDC. Biphasic JNK signaling reveals distinct MAP3K complexes licensing inflammasome formation and pyroptosis. *J Immunol*. 2023;210:167. <https://doi.org/10.4049/jimmunol.210.Supp.167.01>.
58. Otsubo T, Yamada K, Hagiwara T, Oshima K, Iida K, Nishikata K, Toyoda T, Igari T, Nohara K, Yamashita S, Hattori M, Dohi T, Kawamura Y. DNA hypermethylation and silencing of PITX1 correlated with advanced stage and poor postoperative prognosis of esophageal squamous cell carcinoma. *Oncotarget*. 2017;8(48):84434–48. <https://doi.org/10.18632/oncotarget.21375>.
59. Rouco R, Bompadre O, Raueo A, Fazio O, Peraldi R, Thorel F, Andrey G. Cell-specific alterations in Pitx1 regulatory landscape activation caused by the loss of a single enhancer. *Nat Commun*. 2021. <https://doi.org/10.1038/s41467-021-27492-1>.
60. Zhao J, Xu Y. PITX1 plays essential functions in cancer. *Front Oncol*. 2023. <https://doi.org/10.3389/fonc.2023.1253238>.
61. Poos AM, Schroeder C, Jaishankar N, Röhl D, Oswald M, Meiners J, Braun DM, Knotz C, Frank L, Gunkel M, Spilger R, Wollmann T, Polonski A,

- Makrypidi-Fraune G, Fraune C, Graefen M, Chung I, Stenzel A, Erfle H, Rohr K, Baniahmad A, Sauter G, Rippe K, Simon R, Koenig R. PITX1 is a regulator of TERT expression in prostate cancer with prognostic power. *Cancers*. 2022. <https://doi.org/10.3390/cancers14051267>.
62. Song X, Zhao C, Jiang L, Lin S, Bi J, Wei Q, Yu L, Zhao L, Wei M. High PITX1 expression in lung adenocarcinoma patients is associated with DNA methylation and poor prognosis. *Pathol Res Pract*. 2018;214(12):2046–53. <https://doi.org/10.1016/j.prp.2018.09.025>.
63. Wang N, Ma H, Li J, Meng C, Zou J, Wang H, Liu K, Liu M, Xiao X, Zhang H, Wang K. HSF1 functions as a key defender against palmitic acid-induced ferroptosis in cardiomyocytes. *J Mol Cell Cardiol*. 2021;150:65–76. <https://doi.org/10.1016/j.yjmcc.2020.10.010>.
64. Yan Y, He Y, Jiang X, Wang Y, Chen J, Zhao J, Ye J, Lian T, Zhang X, Zhang R, Lu D, Guo S, Xu X, Sun K, Li S, Zhang L, Zhang X, Zhang S, Jing ZJ. DNA methyltransferase 3B deficiency unveils a new pathological mechanism of pulmonary hypertension. *Sci Adv*. 2020;6(50). <https://doi.org/10.1126/sciadv.aba2470>.

Publisher's Note

Springer Nature remains neutral with regard to jurisdictional claims in published maps and institutional affiliations.